Article

Phenotypic Screening-based Identification of 3,4-Disubstituted Piperidine Derivatives as Macrophage M2 Polarization Modulators: An Opportunity for Treating Multiple Sclerosis

qin jie weng, Jinxin Che, Zhikang Zhang, Jiahuan Zheng, Wenhu Zhan, Sendong Lin, Tian Tian, Jincheng Wang, Renhua Gai, Yongzhou Hu, Bo Yang, Qiaojun He, and Xiaowu Dong

J. Med. Chem., **Just Accepted Manuscript** • DOI: 10.1021/acs.jmedchem.8b01635 • Publication Date (Web): 11 Mar 2019

Phenotypic Screening-based Identification of 3,4-Disubstituted Piperidine Derivatives as Macrophage M2 Polarization Modulators: An Opportunity for Treating Multiple Sclerosis

Qinjie Weng,[b,‡] Jinxin Che,[a,‡] Zhikang Zhang,[b,‡] Jiahuan Zheng,[b] Wenhu Zhan,[a] Sendong Lin,[a] Tian Tian,[a] Jincheng Wang,[b] Renhua Gai,[b] Yongzhou Hu,[a] Bo Yang,[b] Qiaojun He,[b] Xiaowu Dong,[a,]*

[a] ZJU-ENS Joint Laboratory of Medicinal Chemistry, Hangzhou Institute of Innovative Medicine, College of Pharmaceutical Sciences, Zhejiang University, Hangzhou, 310058, China

[b] Institute of Pharmacology & Toxicology, Zhejiang Province Key Laboratory of Anti-Cancer Drug Research, College of Pharmaceutical Sciences, Zhejiang University, Hangzhou, 310058, China

‡ These authors contributed equally to this work

KEYWORDS: Multiple sclerosis; Phenotypic screening; Gene biomarker; 3,4-disubstituted piperidine derivative; Macrophage M2 polarization; Modulator

ABSTRACT: Multiple sclerosis (MS) is a disease of the autoimmune-mediated disorder in the central nervous system (CNS), for which no effective therapeutic agent is currently available. The regulation of macrophage polarization towards M2 is a general benefit for treating MS. The gene biomarker-based phenotypic screening approach was developed and 3,4-disubstituted piperidine derivative **S-28** was identified as a lead compound modulating macrophage M2 polarization. Further SAR studies resulted in the discovery of the most potent modulator **D11** that showed good oral bioavailability and significant *in vivo* therapeutic effects. Mechanistic studies demonstrated that the M2 polarization macrophages modulated by **D11** mainly functioned through inhibiting the proliferation of T-cells and activating the phosphorylation of Stat3 and Akt. Therefore, the gene biomarker-based phenotypic screening was demonstrated as a promising tool for the

discovery of novel macrophage M2 polarization modulators. Compound **D11** may serve as a promising starting point for the development of therapeutics to treat MS.

1. Introduction

Multiple sclerosis (MS) represents an immune-mediated chronic and demyelinating disease of the central nervous system (CNS),[1, 2] featuring perivascular leukocyte infiltrates, astrogliosis, axonal damage, and loss of function[3, 4] In particular, MS is the most common cause of neurological disability among young adults, affecting approximately one in 1,000 individuals in both Europe and North America.[5] Clinically, there are various MS treatment approaches available that have been shown to decrease the frequency of relapses and delay disease progression. Examples include beta-interferons, glatiramer acetate, fingolimod, teriflunomide, dimethyl fumarate, natalizumab, and ocrelizumab.[6] However, there is no effective therapeutic agent that cures MS is currently available. Most of the above-mentioned anti-MS drugs only relief the development of MS progression. Moreover, the application of developed anti-MS-drugs is often limited by frequently occurring side effects, including flu-like symptoms and the

development of other autoimmune disorders by interferon-β or fingolimod.[7, 8] Hence, it is of particular importance to identify more effective compounds with new mechanisms of action. Therefore, the development of more effective compounds as alternative approaches for the treatment of MS remains a critical, albeit unmet, scientific goal in MS research.

Macrophages exhibit a dynamic role in host defense and the maintenance of tissue homoeostasis. This necessitates a delicate balance between the proinflammatory and immunomodulatory functions to ensure appropriate responses to environmental stimuli. In general, macrophages can be broadly classified as M1 (classical) and M2 (alternative) subtypes based on function.[9] M1 macrophages are activated by LPS and/or IFN-γ to elaborate proinflammatory cytokine production and tissue inflammation.[10, 11] Conversely, M2 macrophages can be characterized by high expression of arginase 1 (Arg1), mannose receptor C-type 1 (Mrc1), resistin-like molecule alpha1 (Fizz1) on cell surface marker CD206, stimulated by Th2 cytokines IL-4 or IL-13 to promote helminthic immunity, fibrosis, allergy and immunomodulation.[12, 13]

The encephalomyelitis (EAE) model is a standard model for MS.[14] Recently, macrophages have been shown to actively participate in the pathogenesis of EAE progression.[14-16] In particular, during the induction phase of EAE, it was found that the M1 macrophages proportion increases in the spleen, resulting in the draining of lymph nodes (dLNs) in C57BL/6 mice with early EAE.[17] In this state, M1-polarized macrophages were found to exhibit the ability to induce neuronal destruction,[18] with symptoms of ongoing EAE worsening[19]. However, M2-polarized macrophages have been demonstrated to produce pro-repair molecules, including the brain-derived neurotropic factor (BDNF), IL-10, and ferritin.[20-23] After administration of M2-activated macrophages, the development of an EAE model could be significantly suppressed.[24, 25] Importantly, pro-repair molecules secreted by M2 macrophages favor the restoration of myelin and axons, which indicates particularly beneficial characteristics for the potential cure of MS.[26-28] Therefore, the inflammatory phenotype of macrophage cells is crucial for the EAE progression, revealing that the regulatory control of macrophage polarization may be a promising strategy for the treatment of MS. However, the molecular mechanism of regulating macrophages M2-polarization is still not very clear. To the best of our knowledge, there is no specific

effective regulator to treat or control MS using this strategy. Therefore, it would be of particular interest to explore small molecular compounds that could induce the M2-polarization of macrophages for MS therapy.

In recent years, interest in phenotypic screening as a means for small-molecule drug discovery has continued to increase as an alternative to target-based screening.[29, 30] However, there is an ever-growing curiosity to elucidate potential benefits of combining phenotypic and genomic data, in an effort to advance small-molecule drug discovery. Accordingly, the distinct biomarkers of two inflammatory phenotypes (M1 and M2) of macrophage cells described herein render phenotypic screening suitable to find small molecular regulators for macrophages M2-polarization. In previous work, we have established an effective evaluation system of macrophage polarization based on gene biomarkers such as *Arg1* and *Mcp1*.[31] As a continued study for identifying novel macrophage M2 polarization modulators, we wonder whether this evaluation system can be used for the discovery of novel macrophage M2 polarization modulators for the treatment of MS. Thus, similarity search and SAR studies involving different structural moieties of different lead compounds were carried out based on in-house database

screening. This led to the identification of the most potent (both *in vitro* and *in vivo*) compound **D11** (14-folds upregulation of M2 marker *Arg1*). Further mechanism studies of compound **D11** demonstrated that **D11** mainly functioned through inhibiting the proliferation of T-cells in EAE mouse model, and Stat3 and Akt proteins may be important nodes for its regulation of macrophage M2 polarization.

2. Results and Discussion

2.1 Phenotypic screening of a structural diverse compound library

A structurally diverse compound library containing approximately 20,000 compounds was established in-house for phenotypic screening, assisted by cluster analysis. A total of 28 compounds with significantly different structural skeletons were selected (for corresponding compound structures see **Figure S1**). The murine macrophage cell line RAW264.7 was treated with different compounds for 24 hours. Then, the relative expression of macrophage M1 polarization biomarker *Mcp1* and M2 polarization biomarker *Arg1* were tested. As shown in **Figure 1**, several compounds demonstrated a good M2 polarization-inducing activity such as compound **S-2**, **S-7**, **S-9**, **S-11**, **S-13** and **S-28** (for corresponding data see **Table S1**). Specifically, treatment with compound **S-28**

(also termed as PZ8 in our database) was accompanied by the most remarkable elevation of the M2 marker *Arg1* mRNA expression and the least upregulation of M1 marker *Mcp1* mRNA expression among all studied compounds.

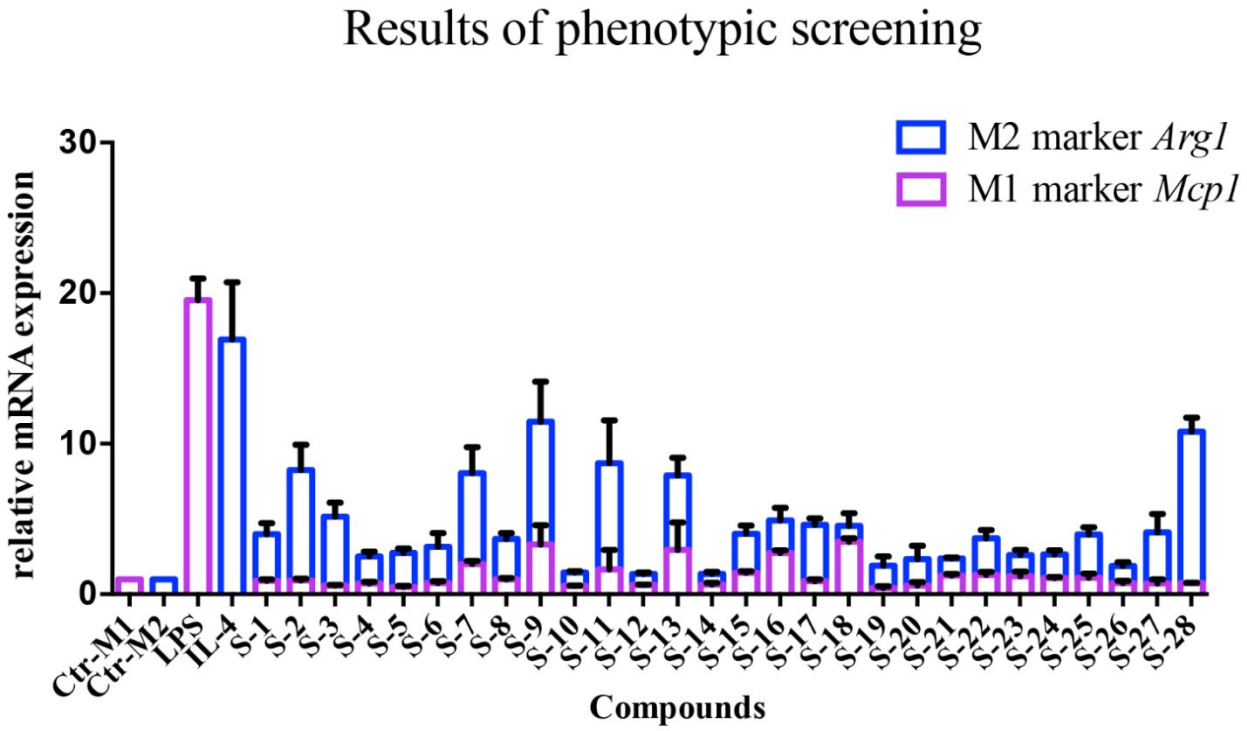

Figure 1. Compound **S-28** promoted macrophages M2 polarization most effectively; (blue) Quantitative real-time polymerase chain reaction (qRT-PCR) analysis for expression of macrophage M2 phenotype gene *Arg1* in RAW264.7 cells treated with 28 compounds (300 nM) for a total 24 hours. IL-4 (20 ng/ml) was used as positive control; (purple) qRT-PCR analysis for expression of macrophage M1 phenotype gene *Mcp1* in RAW264.7 cells

treated with 28 compounds (300 nM) for 24 hours. LPS (50 ng/ml) was used as positive control.

Compound **S-28** (**Figure 2**) was composed of four rings, **a**, **c** and **d** rings represented aryl rings, and the **b** ring represented a saturated (3S, 4S)-piperidine ring. In order to explore the structure-activity relationship of compound **S-28** and in an effort to identify more potent M2 polarization modulators, three strategies were applied: A) A structure similarity search was performed using a Molport database for the purpose of extending the structural diversity based on the skeleton of compound **S-28**; B) It was also found that two chiral centers were present in the **b** ring. Therefore, the influences on M2 polarization modulation activity of the chiral centers was also evaluated; C) In order to explore SAR at the initial stage, the four different ring systems and two rings in compound **S-28** were retained such as the **a**-**b** and **c**-**d** ring systems. Substituted phenyl, heterocycles or saturated chains were selected as substituents of the **a**-**b** or **c**-**d** ring systems.

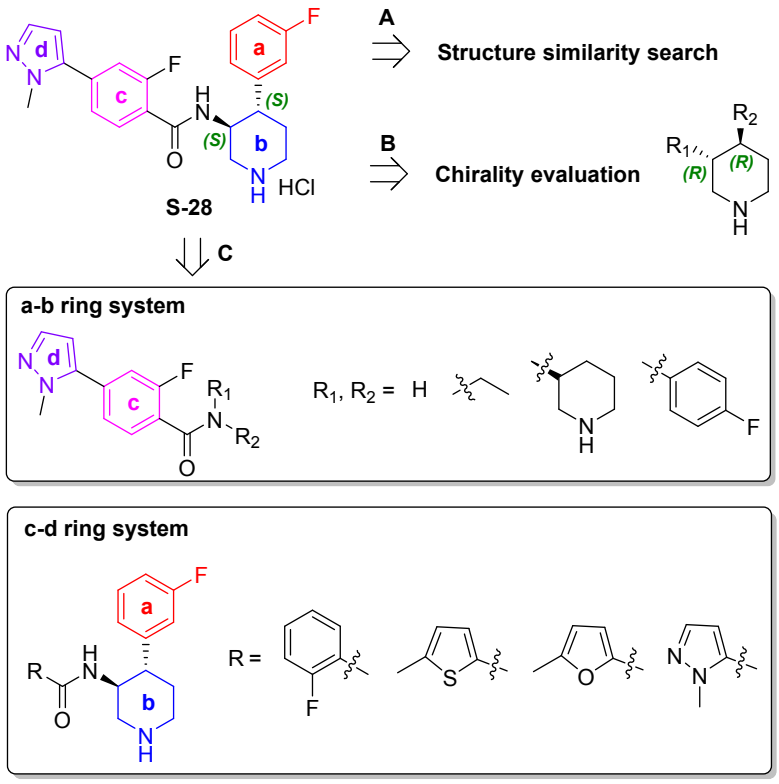

Figure 2. Different strategies of structure modification for SAR study

2.2 The synthetic route of compounds B1, C1-C11 and D1-D21

Synthesis of biaryl carboxylic acid 3a-c, 6a-c, and 9a-j. The synthetic route for the production of the acid fragments is shown in **Scheme 1**. Different esters (**1a-b**, **4**, **7a-d**) were used as starting materials. The coupling reaction with 1-methyl-5-(4,4,5,5-tetramethyl-1,3,2-dioxaborolan-2-yl)-1H-pyrazole provided compounds **2a-b**, **5** and **8a-d**. After electrophilic reaction with NBS or NCS and hydrolysis, the biaryl carboxylic acids **3a-c**, **6a-c** and **9a-j** were obtained.

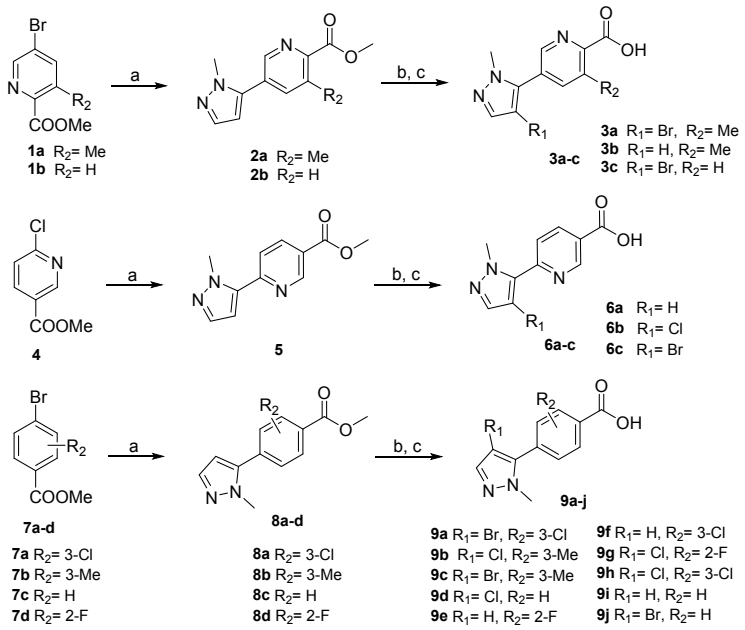

Scheme 1. (a) 1-methyl-5-(4,4,5,5-tetramethyl-1,3,2-dioxaborolan-2-yl)-1H-pyrazole, $Pd(PPh_3)_4$, K_3PO_4, DMF; (b) NBS or NCS, dichloromethane; (c) NaOH, H_2O/EtOH.

Synthesis of 3-amino-4-aryl piperidine 14a-d. The synthetic route to obtain a series of 3,4-disubstituted piperidine compounds is shown in **Scheme 2**. Compounds **10a-c** underwent R or S Jorgensen-Hayashi reagent catalyzed cyclization with compound **10** to provide the (3S,4S) compound **12a-c** and (3R,4R) compound **12d**. Treatment of compound **12a-d** with EtSiH, and following in the presence of Fe/NH_4Cl provided 3-amino-4-aryl piperidine.

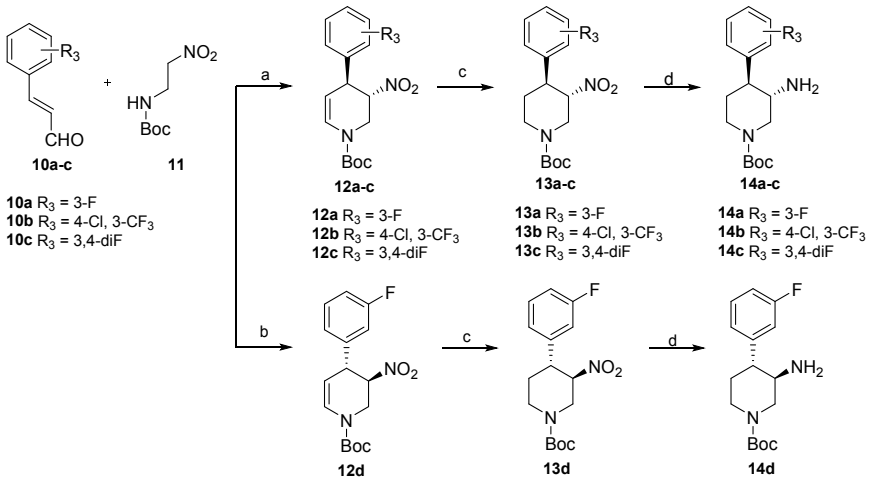

Scheme 2. (a) (S)-2-(diphenyl((trimethylsilyl)oxy)methyl)pyrrolidine, dichloromethane; ii. TFA, dichloromethane; (b) (R)-2-(diphenyl((trimethylsilyl)oxy)methyl)pyrrolidine, dichloromethane; ii. TFA, dichloromethane; (c) i. EtSiH, TFA; ii. Boc_2O, TEA, dichloromethane; (d) Fe, NH_4Cl, $EtOH/H_2O$.

Synthesis of target compounds B1, C1-C11, and D1-D21. The synthetic route for the production of the target compounds is shown in **Scheme 3**. Treatment of aryl acids with aliphatic amines in the presence of EDCI and HOBt provided the condensed intermediates. Then, deprotection with HCl in ethyl acetate yielded the target compounds **B1**, **C1**-**C11**, **D1**-**D19**. For compounds **D20** and **D21**, L-tartrate was introduced to replace hydrochloride as a counteranion. In doing so, the target compounds could be obtained as

white solids as opposed to colorless oils in the case of hydrochloride as a counteranion. The purities of all synthesized compounds were over 95 %.

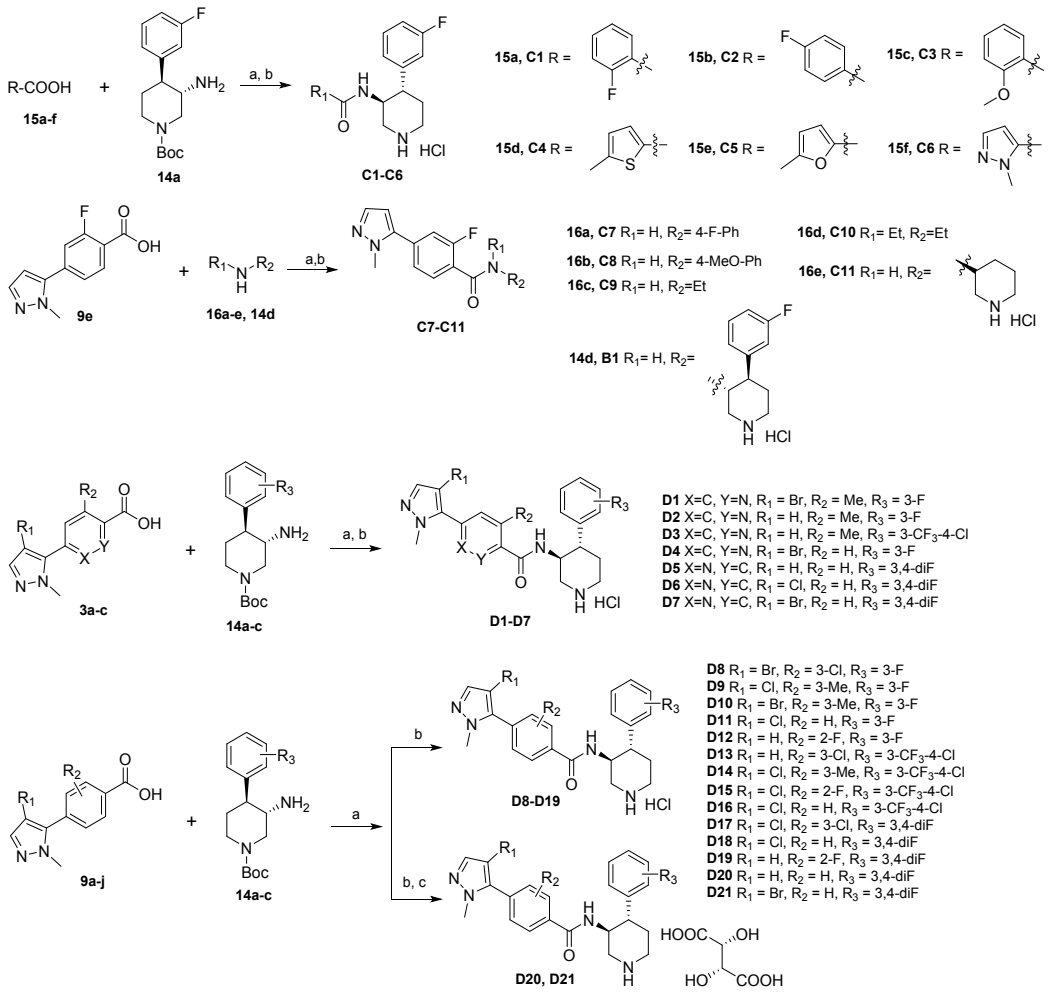

Scheme 3. (a) EDCI, HOBt, DIPEA; (b) EA, HCl; (c) L-Tartaric acid.

2.3 *In vitro* evaluation of macrophage polarization gene biomarker expression fold change

Ten different structures were selected from the Molport database based on similarity search results (**Table 1**). Unfortunately, among these structures, we could not identify any

other more potent skeletons. The bioactivity test results (**Table 1**) indicated that most of the study compounds exhibited low macrophage M2 or M1 polarization induced activity. Specifically, compounds **A2** and **A9** displayed about 4-fold upregulation of *Arg1* expression, however, the activity was significantly lower than that of compound **S-28**.

Table 1. Macrophage polarization gene biomarker expression fold change of compound **A1-A10**

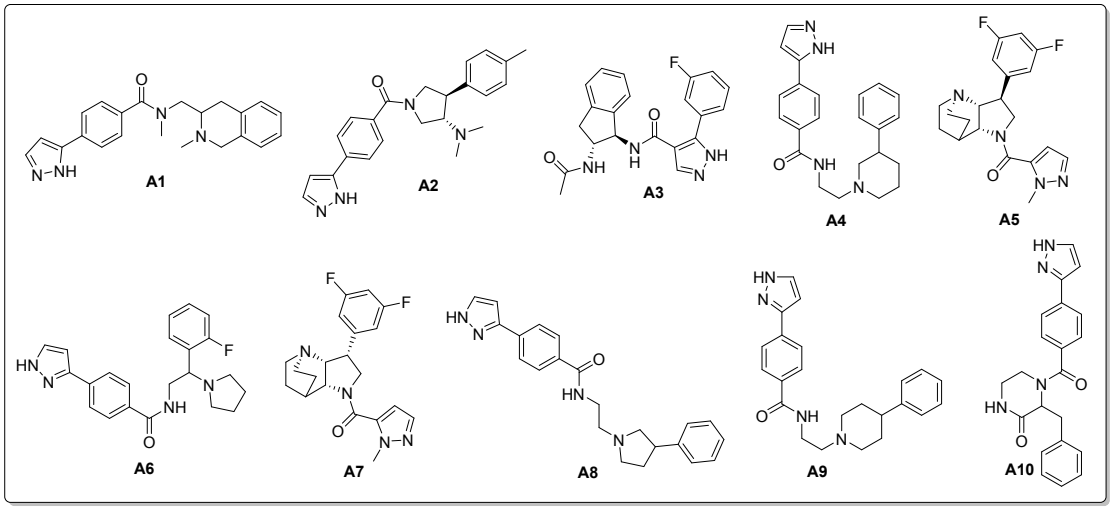

Cpd.	M2 marker Arg1		M1 marker Mcp1	
	Fold[a]	SEM	Fold[a]	SEM
Ctr	1	0	1	0
A1	2.35	0.08	1.14	0.42
A2	4.85	1.04	1.24	0.57

A3	0.80	0.10	2.14	0.66
A4	1.48	0.97	1.52	0.07
A5	1.16	0.26	1.40	0.39
A6	1.09	0.50	1.34	0.05
A7	2.22	0.33	1.95	0.25
A8	2.22	0.45	1.86	0.18
A9	3.92	2.22	2.14	0.33
A10	1.33	0.36	1.53	0.35

[a] Gene expression was determined by qRT-PCR, the fold change was calculated as follows: gene expression level of Dosing group/gene expression level of Control group.

A further study of compound **S-28** focused on chirality and the exploration of other ring systems. As shown in **Table 2**, compound **B1** bearing a (3R,4R)-disubstituted-piperidine ring showed a dramatical loss of M2 polarization induced activity (0.31-fold upregulation of *Arg1*), while the expression of M1 marker *Mcp1* could still be retained (1.76-fold upregulation of *Mcp1*), indicating that the (3S,4S)-disubstituted-piperidine ring was indeed essential in maintaining compound activity.

When the **c**-**d** ring system was replaced by substituted phenyl or heteroaromatic rings such as compound **C1**-**C6**, both exhibited no obvious influences on *Mcp1* expression or

upregulation of *Arg1* expression. As for the **a**-**b** ring system that was replaced by other substituents (compound **C7**-**C11**), the results were performed in the same manner as the lack of the **c**-**d** ring system. The ablation of only the **a** ring (compound **C11**) or the **d** ring (compound **C1**) caused the loss of induced potency. Therefore, we speculated that the a, b, c and d rings were both essential for keeping the induce activity of compound **S-28**.

Table 2. Macrophage polarization gene biomarker expression fold change of compound **B1** and **C1**-**C11**

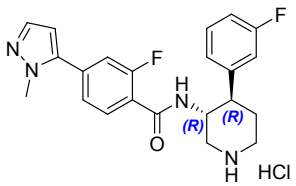

B1

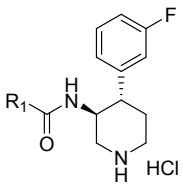

C1-C6

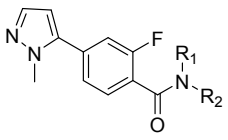

C7-C11

Cpd.	R_1	R_2	M2 marker Arg1		M1 marker Mcp1	
			Fold[a]	SEM	Fold[a]	SEM
Ctr	-	-	1	0	1	0
B1	-	-	0.31	0.14	1.76	0.63
C1		-	1.01	0.43	1.72	0.23
C2		-	0.91	0.24	1.64	0.22
C3		-	1.32	0.28	1.42	0.30

C4		-	1.44	0.36	1.54	0.23
C5		-	1.76	0.68	1.89	0.43
C6		-	1.62	0.17	2.05	0.40
C7	H	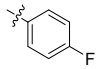	1.63	1.18	2.01	0.33
C8	H	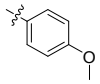	3.86	2.97	2.16	0.19
C9	H	Et	2.31	0.78	1.83	0.31
C10	Et	Et	1.96	0.79	1.97	0.54
C11	H	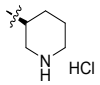	2.11	0.79	2.26	0.56

[a] Gene expression was determined by qRT-PCR, the fold change was calculated as follows: gene expression level of Dosing group/gene expression level of Control group.

The subsequent adjustment of the skeleton was mainly carried out on the substituents of the four rings. When the pyridine ring was substituted for the **b** ring, compound **D1**-**D7** showed no improvements in induced activity (**Table 3**). Based on the above SAR study, we deemed the skeleton highly conserved, and fine-adjustment of compound **S-28** may lead to the identification of an even more potent compound. Compounds **D8**-**D21** were synthesized and tested and the corresponding results are shown in **Table 3**. Compounds **D8**, **D11**, **D12**, and **D15** demonstrated an over 10-fold up-regulation of the M2 marker *Arg1*. As expected, most of the compounds showed less potency in elevating the M1

marker *Mcp1*, except for compounds **D14**-**D16**. Here, R_3 was substituted with 3-CF_3-4-Cl. However, compound **D11** showed the strongest ability to promote expression of the M2 marker *Arg1* in RAW264.7 and much lower upregulation of M1 marker *Mcp1* mRNA expression (**Figure 3A**). Furthermore, RAW264.7 cells were treated with LPS, accompanied by administration of the potent M2 polarization modulators **D8**, **D11**, **D12**, and **D15**. It was found that compound **D11** could also reverse the up-regulation of M1 marker *Mcp1* expression induced by LPS (**Figure 3B**). Thus, compound **D11** was selected for the following pharmacokinetic and pharmacodynamic studies.

Table 3. Macrophage polarization gene biomarker expression fold change of compound **D1-D21**

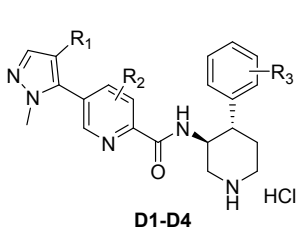

D1-D4

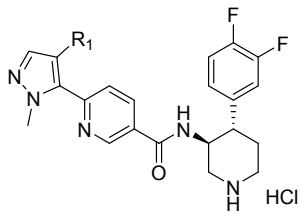

D5-D7

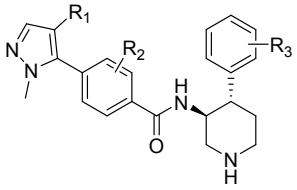

D8-D19 (hydrochloride)
D20, D21 (L-tartrate)

Cpd.	R_1	R_2	R_3	M2 marker Arg1		M1 marker Mcp1	
				Fold[a]	SEM	Fold[a]	SEM
Ctr	-	-	-	1	0	1	0

D1	Br	3-Me	3-F	0.71	0.13	1.63	0.18
D2	H	3-Me	3-F	0.95	0.12	1.99	0.42
D3	H	3-Me	3-CF_3-4-Cl	0.40	0.26	1.37	0.23
D4	Br	H	3-F	0.78	0.26	1.14	0.05
D5	H	-	-	0.85	0.54	1.23	0.05
D6	Cl	-	-	0.27	0.15	1.01	0.04
D7	Br	-	-	0.56	0.08	1.32	0.10
D8	Br	3-Cl	3-F	10.12	0.82	2.05	0.74
D9	Cl	3-Me	3-F	8.35	0.91	2.44	0.76
D10	Br	3-Me	3-F	6.54	1.71	1.89	0.35
D11	Cl	H	3-F	13.97	3.18	1.47	0.12
D12	H	2-F	3-F	10.05	0.92	1.54	0.46
D13	H	3-Cl	3-CF_3-4-Cl	5.08	1.60	1.49	0.32
D14	Cl	3-Me	3-CF_3-4-Cl	1.82	0.01	4.85	0.32
D15	Cl	2-F	3-CF_3-4-Cl	10.33	0.35	3.54	0.77
D16	Cl	H	3-CF_3-4-Cl	2.82	0.51	5.08	0.11
D17	Cl	3-Cl	3,4-diF	1.72	0.23	1.16	0.09
D18	Cl	H	3,4-diF	1.97	0.24	1.50	0.16
D19	H	2-F	3,4-diF	3.99	0.80	0.39	0.15
D20	H	H	3,4-diF	3.42	0.28	0.90	0.24

D21	Br	H	3,4-diF	2.27	0.39	1.77	0.06

[a] Gene expression was determined by qRT-PCR, the fold change was calculated as follows: gene expression level of Dosing group/gene expression level of Control group.

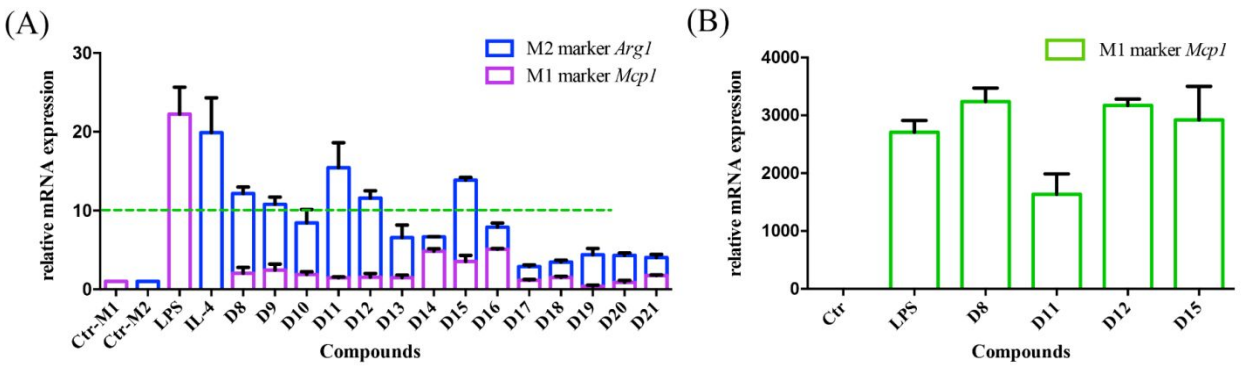

Figure 3. (A) (Blue) qRT-PCR analysis to determine the expression of macrophage M2 phenotype gene *Arg1* in RAW264.7 cells treated with compounds (300 nM) for 24 hours. IL-4 (20 ng/ml) was used as positive control. (Purple) qRT-PCR analysis for the determination of macrophage M1 phenotype gene *Mcp1* expression in RAW264.7 cells treated with compounds (300 nM) for 24 hours. LPS (50 ng/ml) was used as positive control; (B) qRT-PCR analysis for the determination of macrophage M1 phenotype gene *Mcp1* expression. RAW264.7 cells were pre-treated with LPS (50 ng/ml) for 24 hours and subsequently treated with compounds (300 nM) for 24 hours. Data is shown as mean ± S.E.M in the graphs.

2.4 *In vivo* pharmacokinetic evaluation

Definitive single-dose pharmacokinetic studies were conducted in rats (**Table 4**). Compound **D11** demonstrated excellent absolute oral bioavailability in rats with F values of 50.63%. In addition, the compound showed good clearance and oral absorption ($t_{1/2}$= 3.3 h, C_{max}= 313 ng/mL, AUC_{0-t}= 4669 μg /L·h) characteristics. These data suggested that compound **D11** constitutes a reasonable starting point for further drug development studies.

Table 4. Pharmacokinetic parameters of **D11** in Sprague-Dawley (SD) Rat

Parameters	Compound **D11**	
	50 mg/kg	10 mg/kg
	Oral	Intravenous
T_{max}（h）	3.25±0.5	0.083±0.02
$T_{1/2}$（h）	7.77±1.52	6.30±1.90
C_{max}（μg/L）	313.23±87.45	1001.40±423.30
AUC_{0-t}(μg /L·h)	4669.27±1165.37	1844.42±568.57
$AUC_{0-\infty}$(μg /L·h)	4743.69±1166.54	1869.93±585.16
R_AUC $_{(t/\infty)}$%	98.425±1.32	98.75±1.287

F	50.63%

2.5 Compound D11 changes macrophage polarization balance towards M2

In **D11**-treated RAW264.7 cells, the microarray analysis result indicated that **D11** activated M2 macrophage marker genes but suppressed M1 marker genes (**Figure 4A**, **B**). Compared to the passage cell line RAW264.7, bone marrow-derived macrophages (BMDM) present a more ideal *in vitro* model to understand the mechanisms controlling polarization of activated macrophages.[32] It was further demonstrated that the M2 macrophages marker CD206 expression was elevated (**Figure 5A**) and M1 macrophages marker CD86 expression was suppressed dose-dependently after treatment with **D11** (**Figure 5B**) on BMDMs.

Hence, the BMDM cell line was used for further bio-mechanistic studies of compound **D11**. Treatment of BMDMs with 300 nM **D11** resulted in an increase of mRNA levels of the M2 markers *Arg1, Mrc1, Fizz1* (**Figure 4C**). Furthermore, compound **D11** at a concentration of 300 nM reversed the elevation of mRNA levels of the M1 markers *Mcp1,*

Inos and *Cd86* stimulated by LPS (**Figure 4D**). Meanwhile, the western blot analysis also showed that the expression level of macrophage M2 polarization marker Arg1 and Ym1 proteins increased while the M1 polarization marker Tnf-α protein was still remained (**Figure S2**). Furthermore, treatment of BMDM cells with 300 nM of **D11** increased the expression of the M2 macrophages marker CD206 (**Figure 4E**) and suppressed the expression of the M1 macrophages marker CD86 stimulated by LPS (**Figure 4F**) as measured by flow cytometry.

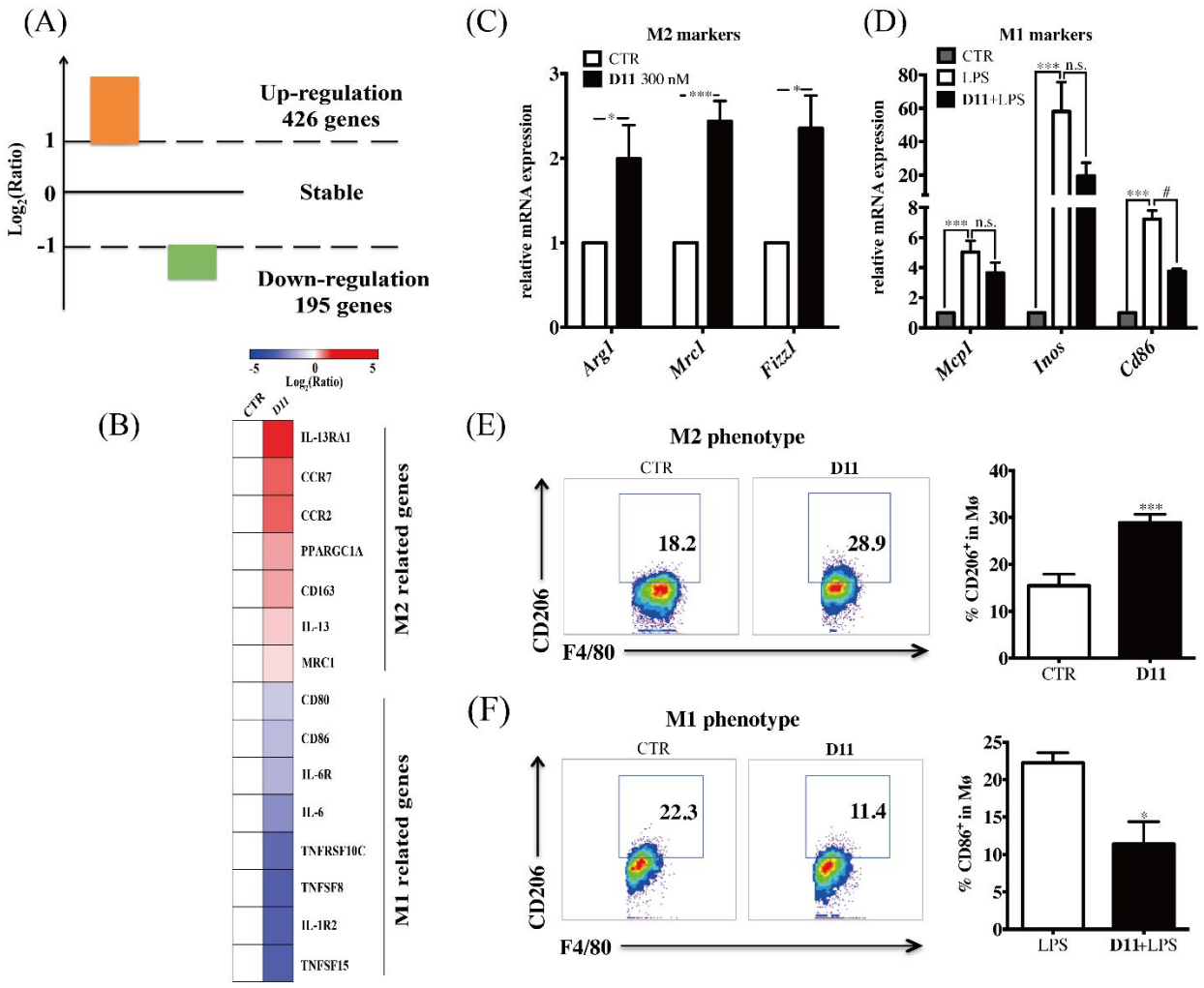

Figure 4. Compound **D11** promotes the polarization of M2 macrophages in combination with inhibiting M1 polarization *ex vivo*. (A) The numbers of altered genes after the RAW264.7 cells were treated with **D11**; (B) Fold change of macrophage polarization gene markers; (C) BMDM cells were treated with 300 nM of **D11** for 24 hours. qRT-PCR was performed to investigate the macrophages M2 polarization-associated genes *Arg1*, *Mrc1*, and *Fizz1* mRNA expression levels. (D) BMDM cells were pre-treated with LPS (50 ng/ml)

for 24 hours and then treated with 300 nM of **D11** for 24 hours. qRT-PCR was performed to investigate the macrophages M1 polarization-associated gene *Mcp1*, *Inos*, *Cd86* mRNA expression levels. (E) BMDM cells were treated with 300 nM of **D11** for 24 hours. The percentage of M2 macrophages ($CD206^+F4/80^+$ cells) was analyzed by flow-cytometry. (F) BMDM cells were pre-treated with LPS (50 ng/ml) for 24 hours and then treated with 300 nM of **D11** for 24 hours. The percentage of M1 macrophages ($CD86^+F4/80^+$ cells) was analyzed by flow cytometry. Data is shown as mean ± S.E.M in the graphs. *P<0.05, ***P<0.01 versus control.

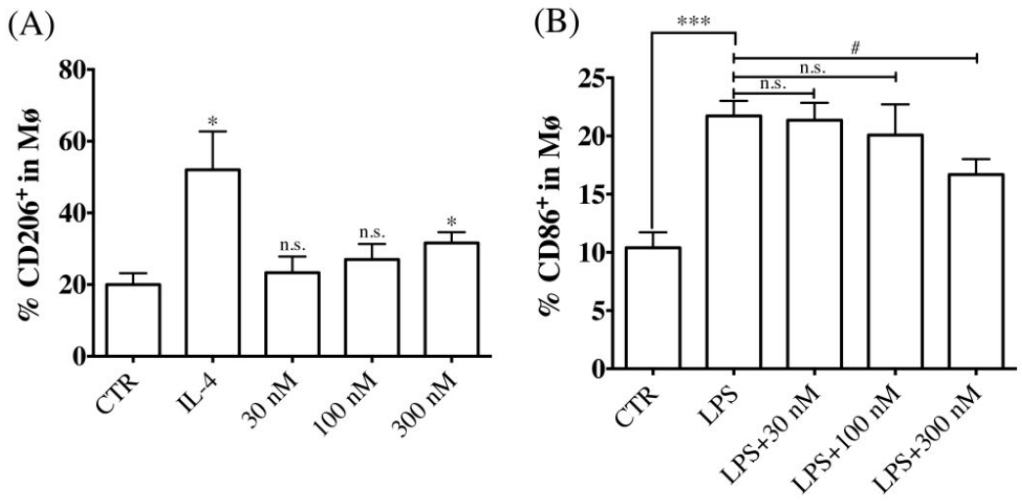

Figure 5. D11 promotes macrophages M2 polarization and inhibits M1 polarization dose-dependently. (A) BMDM cells were treated with indicated concentration of **D11** for 24

hours. The percentage of M2 macrophages ($CD206^+F4/80^+$ cells) was analyzed by flow-cytometry. (B) BMDM cells were pre-treated with LPS (50 ng/ml) for 24 hours and then treated with indicated concentration of **D11** for 24 hours. The percentage of M1 macrophages ($CD86^+F4/80^+$ cells) was analyzed by flow cytometry. Data is shown as mean ± S.E.M in the graphs. *P<0.05, ***P<0.01 versus control group. #P<0.05 versus LPS group. n.s. P>0.05 versus control or LPS group.

2.6 Therapeutic effect of compound D11 in EAE model

Since the Myelin Oligodendrocyte Glycoprotein (MOG) has emerged as one of the most important target antigens in MS,[14] the *in vivo* therapeutic effect of compound **D11** was evaluated in a MOG_{35-55} induced mouse EAE model. Further safety evaluation of **D11** on healthy mice indicated that no other obvious side effects were observed except for immunosuppressive activity (which is beneficial in EAE and MS) at 400 mg/kg (**Figure S3**, **Table S2**, and **S3**). To avoid the potential side effects caused by excessive immunosuppression and maintain the exposure of **D11** being above 300 nM, the doses of 100 mg/kg and 200 mg/kg were chosen as the therapeutic doses in animal EAE study.

The therapeutic administration of the drug (**D11**, 100 mg/kg and 200 mg/kg, ig, qd) was performed after day 8, right after the appearance of clinical symptoms of EAE (**Figure 6A**). Dexamethasone (DXM), which is the first choice for the treatment of acute relapses of multiple sclerosis,[33] was also observed therapeutic effect in the EAE model when treating with dexamethasone as reported,[34] so it was chosen as a positive control. The data indicated that when administered at 200 mg/kg, compound **D11** clearly reduced disease progression, as observed by a significantly lower average clinical score in EAE mice administrated with 200 mg/kg of compound **D11** compared to vehicle-treated EAE mice (**Figure 6B**). Accordingly, H&E and LFB histological analysis of the affected spinal cord indicted that treatment with 200 mg/kg of **D11** attenuated demyelination and inflammation in EAE mice (**Figure 6C** and **D**). To study the effect of treatment with compound **D11** on the pro-inflammatory cells Th1, and Th17 infiltration into the CNS, we isolated mononuclear cells (MNCs) from the CNS (spinal cords and brains) of EAE mice. Then, we performed flow-cytometry analysis and detected a remarkable percentage reduction of both Th1 and Th17 in $CD4^+$ T-cells of **D11**-treated EAE mice (**Figure 6E** and **F**).

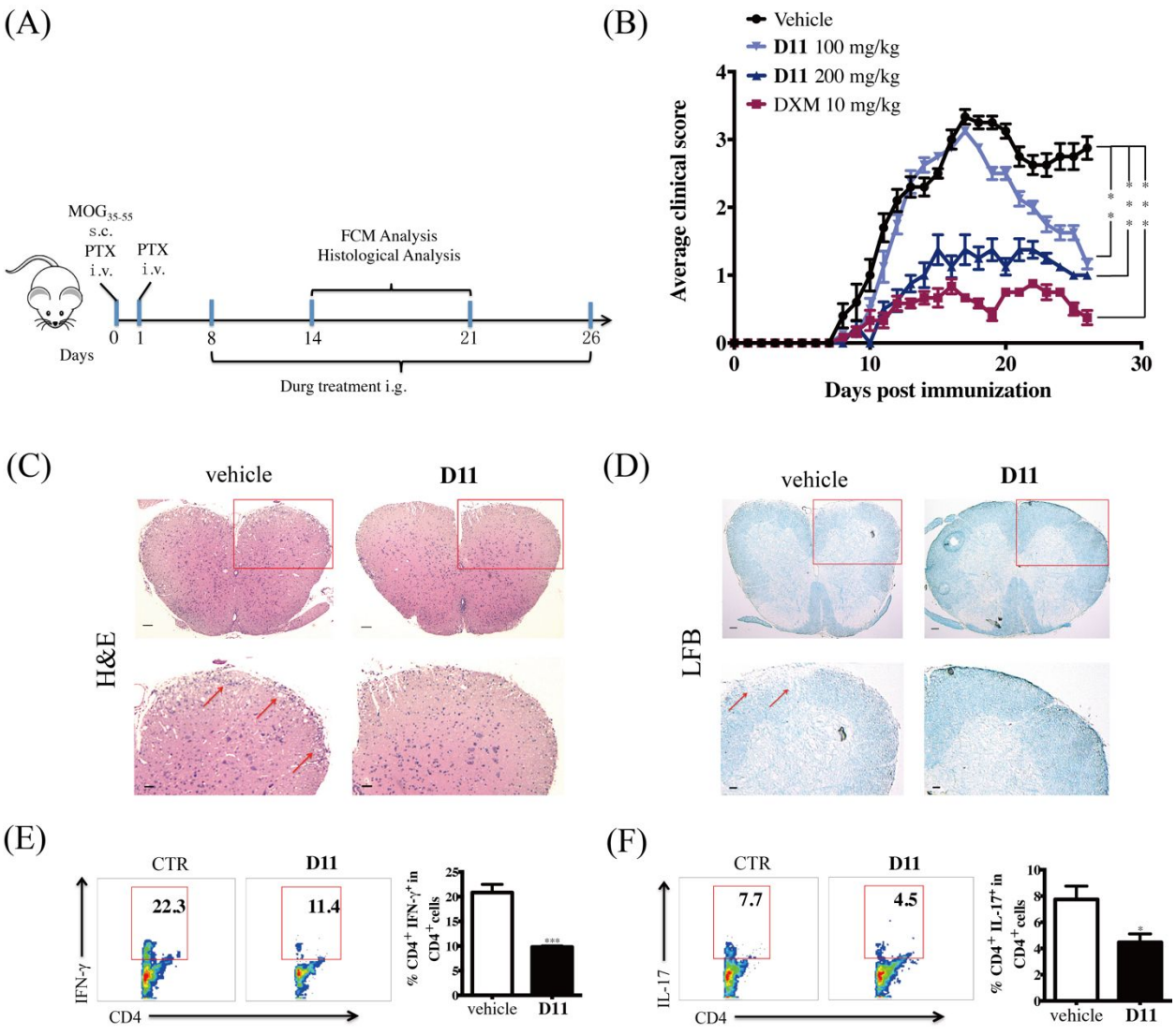

Figure 6. Compound **D11** ameliorated clinical severity and limited CNS autoimmunity of EAE mice. (A) Schematic representation of EAE model. (B) *In vivo* effect of compound **D11** on EAE mice. EAE mice were treated with **D11** (100 mg/kg, 200mg/kg, i.g.), dexamethasone (10 mg/kg, i.g.) or vehicle (saline, i.g.). Mean clinical scores are shown (n=5). (C,D) H&E and Luxol fast blue (LFB) staining of spinal cords from vehicle- and

D11-treated EAE mice on day 14 after induction of EAE. The shown arrows indicate infiltration of inflammatory cells and demyelination in the spinal cord. Scale bars: 100 μm (upper), 50 μm (bottom). (E, F) Flow cytometry analysis of Th1 and Th17 (IFN-γ$^+$ and IL-17$^+$) on the range of CD4$^+$ cells isolated from the CNS of vehicle-treated and 200 mg/kg **D11**-treated EAE mice (n=4 mice per group), detected between day 13 to day 19 after induction of EAE. Data is shown as mean ± S.E.M in the graphs. *P<0.05, **P<0.01, ***P<0.01 versus vehicle control.

2.7 Compound D11 distorts macrophages polarization towards M2 *in vivo*

To evaluate the *in vivo* effect of compound **D11** on modulating the polarization of macrophages, flow cytometry was used to assess the polarization of macrophages in EAE mice between day 13 to day 19 after induction of EAE. As shown in **Figure 7A**, the proportion of M2 macrophages (F4/80$^+$CD206$^+$) in total macrophage populations (F4/80$^+$) from both peripheral immune organs (spleen and draining lymph nodes) and the CNS (spinal cord and brain) was found to be significantly elevated in 200 mg/kg **D11**-treated mice compared to vehicle-treated EAE mice. Conversely, the percentage of M1

macrophages ($F4/80^+CD86^+$) in total macrophage populations ($F4/80^+$) was found to be declined in 200 mg/kg **D11**-treated mice compared with vehicle-treated EAE mice (**Figure 7B**). In addition, the influence on dendritic cells and T_{reg} cells wasn't observed in **D11**-treated EAE mice (**Figure S4**).

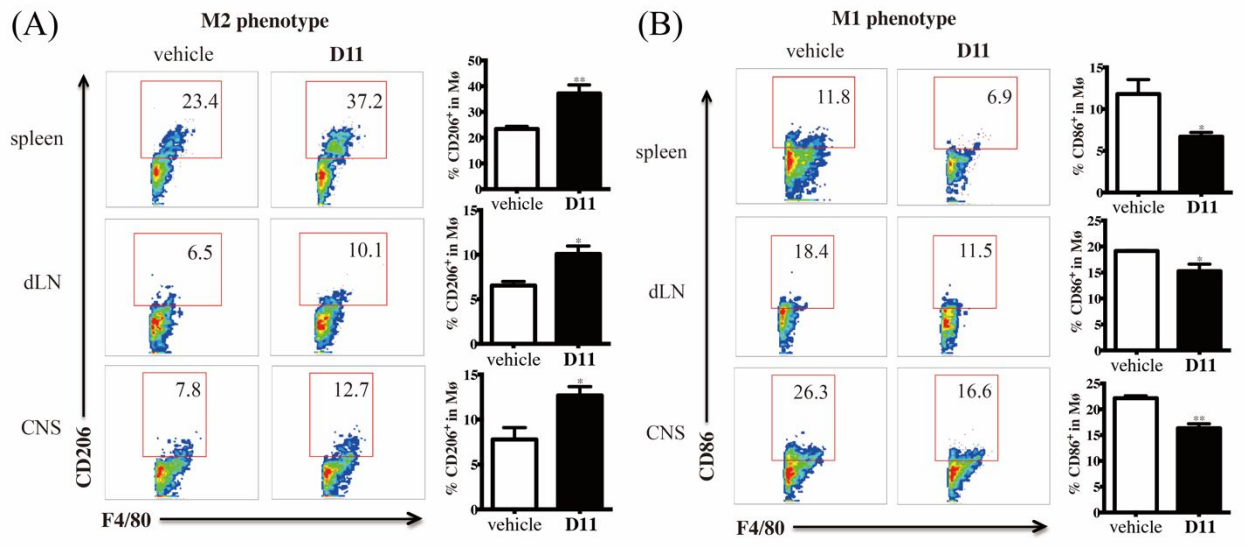

Figure 7. Compound **D11** promotes polarization of M2 macrophages and inhibits M1 polarization in EAE mice. (A, B) Spleen, DLN and CNS were isolated from vehicle-treated and **D11**-treated (200 mg/kg) EAE mice (n=4 mice per group) between day 13 to day 19 after induction of EAE. (A) Flow cytometry analysis of M2 marker CD206 in the range of macrophage marker $F4/80^+$ cells. (B) Flow cytometry analysis of M1 marker CD86 in the

range of macrophage marker F4/80^{+} cells. Data is shown as mean ± S.E.M in the graphs. *P<0.05, **P<0.01 versus control.

2.8 Studies of compound D11 on crosstalk between macrophages and CD4+ T cells

Our data indicated that treatment with compound **D11** altered the polarization of macrophages towards an anti-inflammatory phenotype. We then addressed the issue of functionality of **D11**-treated macrophages. As a potent member of the myeloid lineage, during the induction phase of EAE, M1 macrophages adapt an antigen presenting cell (APC)-like capacity to active CD4+ T cells proliferation and differentiation.[35] Importantly, compound **D11** suppressed M1 macrophages-driven T-cell proliferation (**Figure 8A** and **B**). Furthermore, **D11**-treatment decreased the production of the Th1 and Th17 cell signature cytokines IFN-γ and IL-17A (**Figure 8C** and **D**).

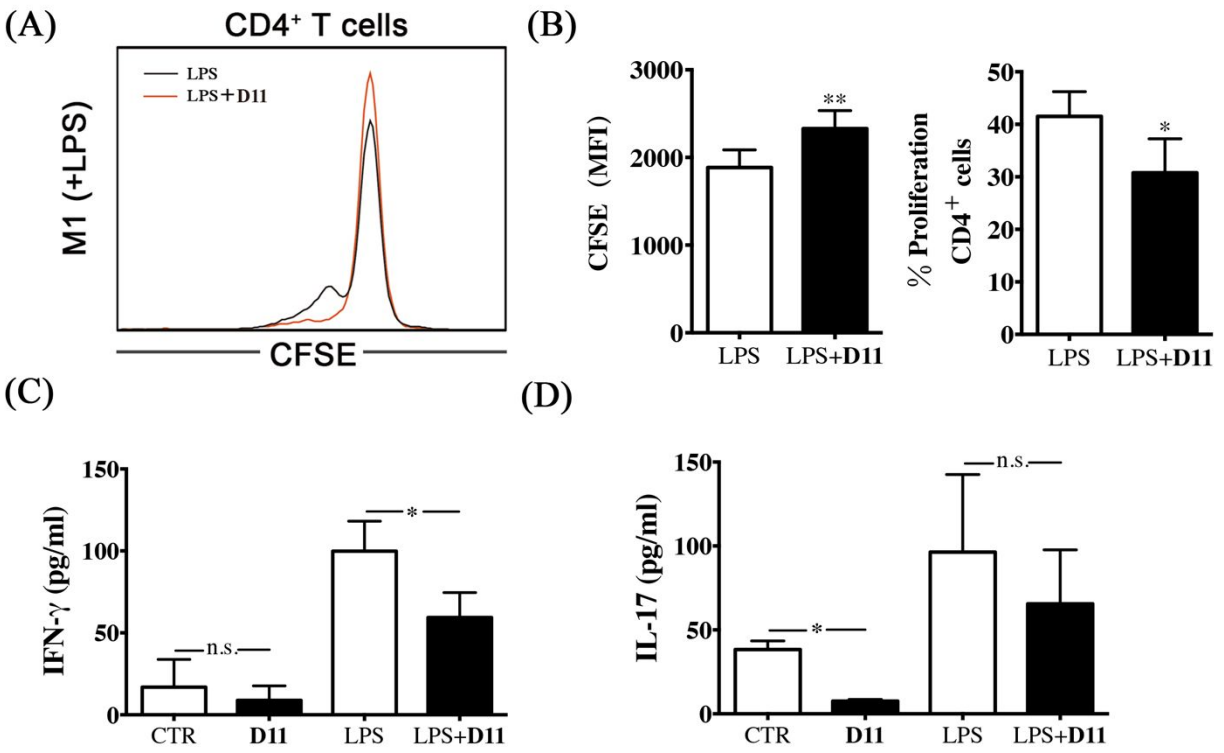

Figure 8. **D11**-treated macrophages inhibited the proliferation of CD4+ T cells. (A, B) BMDM cells were treated with 50 ng/ml LPS or with 300 nM of compound **D11** for 48 hours. Then, BMDM cells were co-cultured with CD4+ T cells and proliferation was determined after 72 hours. Histograms display proliferation profiles of CD4+ T-cells. Graphs display mean fluorescence intensity (MFI) of the proliferation dye CFSE and proliferation percentages of CD4+ T-cells. (C, D) Co-culture supernatant was collected for ELISA analysis of IFN-γ and IL-17 secretion. Data is shown as mean ± S.E.M in the graphs. *P<0.05, **P<0.01, n.s. P>0.05 versus control.

2.9 Compound D11 promotes macrophages polarization via activating Akt/Stat3 pathways

In order to fully comprehend the mechanisms involved in the processes described above, microarray analysis was performed using a gene chip technology. RAW264.7 cells were treated in the absence or presence of 300 nM of compound **D11** for 24 hours. Among the altered genes (2729 upregulated vs. 2769 downregulated, **Figure 9A**), the potential target genes in response to **D11** treatment were listed in **Figure 9B**, which could well explain the mechanism of macrophages M2 polarization. A number of TLR ligands and cytokines such as TLR4 and IL-6 are potent macrophages M1 polarization promoters, which lead to activation of pro-inflammatory transcription factor STAT1 and NF-κB.[36] Cytokine IL-4 activated Stat6 and IL-10 activated Stat3, which in turn activated transcription of genes typical of M2 polarization, e.g., mannose receptor (Mrc1), resistin-like α (Retnla, Fizz1), chitinase 3-like 3 (Chi3l3,Ym1), IL-10 and TGF-β.[37, 38] Among all altered genes, Kyoto Encyclopedia of Genes and Genomes (KEGG) pathway classification analysis[39, 40] showed that the genes of the immune system and signal transduction were the most altered (**Figure 9C**). Based on the microarray analysis results,

we further found that the significantly differentially expressed (SDE) genes such as IKK, Pim-1, AMLI-ETC, and PML-RARα proteins mainly belonged to the Jak-Stat and PI3K-Akt signaling pathway (**Figure S5**). Subsequently western blot analysis was performed as shown in **Figure 9D**. Compound **D11** was demonstrated to promote phosphorylation of Akt at both sites of 308 and 473, and phosphorylation of Stat3, but didn't influence phosphorylation of Stat6. This finding is believed to be due to Stat3 and Akt protein representing an important node in modulating macrophage M2 polarization after treatment with compound **D11**.

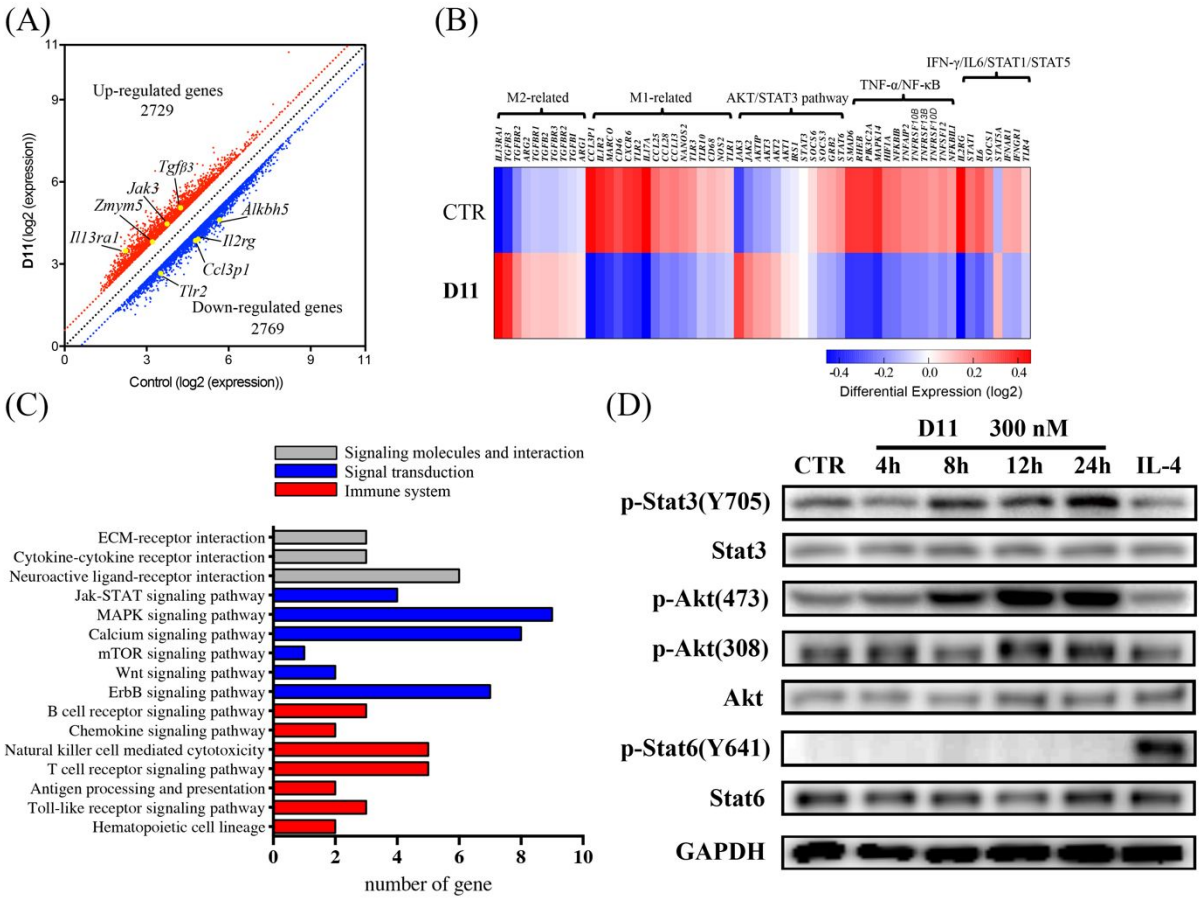

Figure 9. (A) Volcano plot of differentially expressed genes by microarray analysis on **D11** treated macrophages Raw 264.7. (B) Heatmap of differentially expressed genes by microarray analysis on **D11** treated macrophages Raw 264.7. (C) Changes of gene expression in the KEGG pathway analysis. (D) Western blotting shows the expression level of Akt/p-Akt(473)/p-Akt(308), Stat3/p-Stat3(Y705) and Stat6/p-Stat6 protein, GAPDH was used as loading control.

3. Conclusions

Macrophages exhibit important roles in the development of MS. M1 polarization macrophages exert pathogenic effects while M2 polarization macrophages present an anti-inflammatory phenotype. Thus, molecular intervention to alter macrophages polarization towards M2 poses as a potential therapeutic approach for the treatment of MS. Compound **S-28** bearing a 3,4-disubstituted piperidine skeleton was identified from an in-house compound library by using phenotypic screening. Following medicinal chemistry optimization and SAR studies revealed compound **D11** as the most potent derivative in this series that altered macrophages M2 polarization, together with excellent oral bioavailability and therapeutic effects in a mural EAE model. It was also found that compound **D11** was able to distort the polarization of macrophages towards M2 *in vivo*, and M2 polarization macrophages functioned through inhibiting T-cell proliferation. According to gene chip and western blot studies, Stat3 and Akt proteins were identified to be the main targets that contributed to the biological effects induced by the treatment of compound **D11** (**Scheme 4**). As previously reported, the PI3K/Akt signaling pathway plays a vital role in mediating the macrophages polarization,[41-43] and p-STAT3 is a strong transcription factor of many M2-related genes.[36] Whereas we only proved that Akt and

Stat3 phosphorylation are involved in **D11** promoting macrophage M2 polarization, further study is needed to investigate the synergistic role of Akt and Stat3 in macrophages M2 polarization. Our study not only demonstrated a promising approach for the discovery of novel macrophage M2 modulators for the treatment of MS but also provided a new strategy for phenotypic screening of modulators that could alter cells in different states. Compound **D11** identified in this study may be taken as a promising starting point for the development of small molecule therapeutics to treat MS.

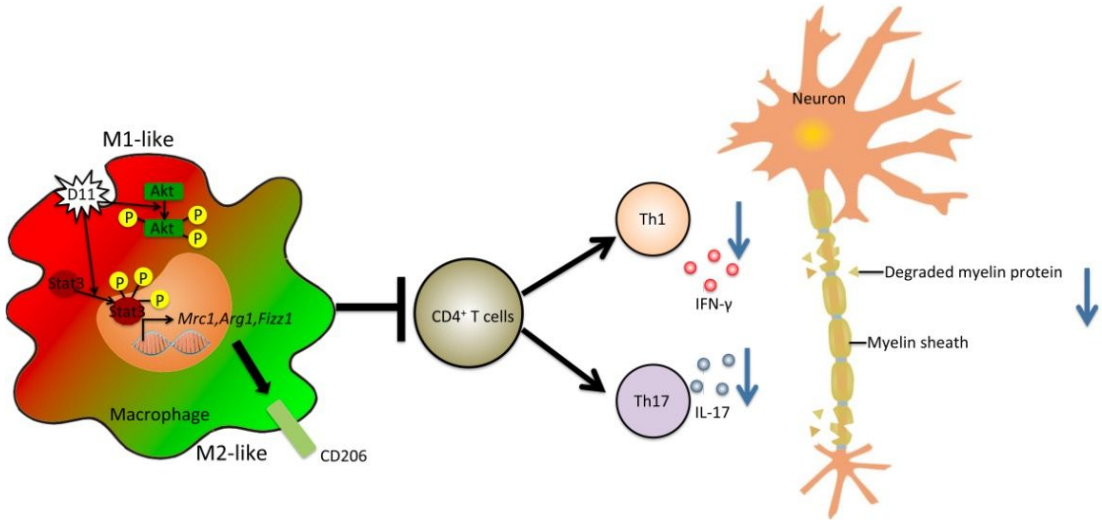

Scheme 4. Schematic representation of **D11**-mediated M2 polarization and neuroprotective effect. **D11** is uptaken by macrophages and promotes macrophages M2 polarization by activating Akt and Stat3. Phosphorylated Stat3 translocated into the

nucleus encoding M2 macrophages related genes such as *Mrc1*(CD206), *Arg1* and *Fizz1*. **D11**-treated macrophages inhibit CD4+ T cells proliferation, therefore reduce the inflammatory reaction generated by autoreactive Th1 and Th17 cells, finally inhibits demyelination and prevents of EAE.

4. Experimental Section

Chemistry

^{1}H NMR and ^{13}C NMR spectra were recorded at 500 MHz using a Bruker AVANCE III spectrometer in $CDCl_3$, or DMSO-d_6 solution, with tetramethylsilane (TMS) serving as the internal standard. Chemical shift values (δ) were reported in ppm. Multiplicities are recorded by the following abbreviations: s, singlet; d, double; t, triplet; q, quartet; m, multiplet; J, coupling constant (Hz). High-resolution mass spectrum (HRMS) were obtained from Agilent Technologies 6224 TOF LC/MS. The purities of compounds for biological testing were assessed by NMR and HPLC, and the purities were ≥95 %. The analytical HPLC was performed on an Agilent 1260 Infinity II (LC03) machine and a C18 reversed-phase column (Agilent Eclipse XDB-C18, 4.6*250 mm, 5 μm), with a flow rate

of 1.0 mL/min, the detection by UV absorbance at a wavelength of 254 nm, the column temperature was 25 ℃, eluting with water (0.1% trifluoroacetic acid) as A phase and methanol as B phase (0 min, A phase: 90%, B phase: 10%; 8 min, A phase: 10%, B phase: 90%; 13 min, A phase: 10%, B phase: 90%; 15 min, A phase: 90%, B phase: 10%; 20 min, A phase: 90%, B phase: 10%). Unless otherwise noted, reagents and solvents were obtained from commercial suppliers and without further purification.

General procedure A: (for the synthesis of compounds **2a**, **2b**, **5**, **8a-d**) Tetrakistriphenylphosphane Pd (0) (3.45 g, 3 mmol) was added to a stirred suspension of 4-halogen-substituted aromatic ester (30 mmol), 1-methyl-5-(4,4,5,5-tetramethyl-[1,3,2] dioxaborolan-2-yl)-1H-pyrazole (7.5 g, 36 mmol) and potassium phosphate (12g, 45 mmol) in dimethylformamide (100 mL) at 0 °C under nitrogen protection. The reaction mixture was heated at 100 °C for 10 h, then poured into H_2O (300 mL) and extracted with ethyl acetate (100 mL × 3). The combined organic layers were washed with saturated brine (200 mL × 3), dried over Na_2SO_4, and concentrated under vacuum to afford an off-white semisolid. The crude product was purified by column chromatography.

General procedure B: (for the synthesis of compounds **3a**, **3c**, **6b**, **6c**, **9a-d**, **9g**, **9h**, **9j**) To a solution of biaryl ester (10mmol) in dry THF/DMF (v/v, 10: 1) at 0 °C was added NCS (1.46 g, 11 mmol) in one portion. The reaction mixture was stirred at r.t. for 5 h. After it was fully reacted, the mixture was poured into H_2O (50 mL) and extracted with ethyl acetate (30 mL × 3). The combined organic layers were washed with saturated brine (50 mL × 2), dried over Na_2SO_4 and concentrated under vacuum. The residue was purified by column chromatography.

To a solution of the above intermediate products (8.8 mmol) in dry THF/EtOH (v/v, 4: 1) was slowly added aqueous NaOH (3 N, 10 mL, 30 mmol) and the mixture was stirred at r.t. for 5 h. After it was fully reacted, the solvent was removed under vacuum and the resulting crude mixture was dissolved in H_2O (30 mL) and acidified with 1 N hydrochloric acid until pH 2~3, and extracted with ethyl acetate (30 mL × 3). The combined organic layers were washed with saturated brine, dried over anhydrous Na_2SO_4, and then concentrated to dryness under vacuum to provide the white solid.

General procedure C: (for the synthesis of compounds **3b**, **6a**, **9e**, **9f**, **9i**) To a solution of biaryl ester (2.2g, 8.8mmol) in the mixture of tetrahydrofuran and ethanol (v/v = 4:1,

30mL), aqueous NaOH (3N, 10mL, 30mmol) was slowly added. The mixture was stirred at r.t. for 5h. The mixture was then concentrated under reduced pressure, the residue was resolved in water (30 mL) and acidified with 1 N hydrochloric acid until pH 2 ~ 3 and extracted with ethyl acetate (30 mL × 3). The combined organic layers were washed with saturated brine, dried over anhydrous Na_2SO_4, and dried under vacuum to afford the white solid.

General procedure D: (for the synthesis of compounds **12a-d**) To a solution of compound **11** (*tert*-butyl-(2-nitroethyl) carbamate, 285 mg, 1.5 mmol), (2S) or (2R)-2-(diphenyl((trimethylsilyl)oxy)methyl) pyrrolidine (33 mg, 0.1 mmol) and benzoicacid (25 mg, 0.2 mmol) in dry dichloromethane (2 mL) was slowly added substituted cinnamyl aldehyde (1 mmol) at 0 °C. After the addition was complete, the reaction was warmed up to room temperature and stirred overnight. The stirring was continued until aldehyde was consumed (monitored by TLC). The solution was diluted to 10 mL with dichloromethane and trifluoroacetic acid (148 μL, 2 mmol) was added dropwise, then the reaction mixture was stirred for another 5 h. The reaction was quenched by the dropping of 1N aqueous sodium bicarbonate solution (10 mL) and stirred for another 10 min. Water phase was

extracted with ethyl acetate (10 mL × 3), and the combined organic layers were washed with saturated brine (20 mL × 2) dried over anhydrous sodium sulfate and concentrated. Purification by flash column chromatography afforded yellow solid.

General procedure E: (for the synthesis of compounds **13a-d**) To a solution of 3,4-disubstituted piperidine compound (5.4 mmol), triethylsilane (1.8 mL, 11 mmol) in dichloromethane (25 mL) was added dropwise trifluoroacetic acid (3.7 mL, 50 mmol) at 0 °C. After the addition was complete, the reaction was warmed up to room temperature and stirred overnight. Then the reaction was quenched by the dropping of saturated aqueous sodium bicarbonate (50 mL) and stirred for another 10 min. Water phase was extracted with dichloromethane (20 mL × 3), and the combined organic layers were washed with saturated brine (20 mL × 2) dried over anhydrous sodium sulfate and concentrated in vacuo to give an oil. To a suspension of the residue and triethylamine (1.4 mL, 10 mmol) in tetrahydrofuran (45 mL), di-*tert*-butyl dicarbonate (3.7 mL, 50 mmol) was added in batches at 0 °C. After the addition was complete, the reaction was warmed up to room temperature and stirred for 5 h. After solvent removal, the residue was dissolved in ethyl acetate (50 mL), washed by 0.5N hydrochloric acid (20 mL × 2) and

saturated brine (20 mL × 2) and dried over anhydrous sodium sulphate. After solvent removal, the residue was purified by column chromatography to afford the product as a white solid.

General procedure F: (for the synthesis of compounds **14a-d**) To a suspension of 3,4-disubstituted piperidine compound (4.2 mmol) in ethyl alcohol - water (v/v, 3: 1, 40mL) was added iron powder (2.82 g, 50.4 mmol) and ammonium chloride (1.0 g, 16.8 mmol), then the mixture was refluxed for 5 h with mechanical stirring. After it is fully reacted, the mixture was filtered and filtrate was concentrated under vacuum. The residue was dissolved in ethyl acetate (50 mL), washed by saturated aqueous sodium bicarbonate (20 mL × 2) and saturated brine (20 mL × 2) and dried over anhydrous sodium sulphate. After solvent removal, the residue was dried in vacuum to give gray solid.

General procedure G: To a suspension of the acid (0.2 mmol), EDCI (69 mg, 0.36 mmol), HOBT (49 mg, 0.36 mmol) and DIPEA (87 μL, 0.5 mmol) in dichloromethane was added the amine (58.8 mg, 0.2 mmol), then the mixture was reacted for 5 h at room temperature with mechanical stirring. After it was fully reacted, the mixture was concentrated under vacuum. The residue was dissolved in ethyl acetate (50 mL), washed

by 1N HCl (20 mL × 2) and saturated brine (20 mL × 2) and dried over anhydrous sodium sulphate. After solvent removal, the residue was purified by column chromatography to afford the product as light-yellow solid (for the synthesis of compounds **C7**-**C10**).

To a solution of the above yellow solid in ethyl acetate was added HCl saturated ethyl acetate, stirred at room temperature for 6 h. After it was fully reacted, the mixture was filtered, the resulted solid was washed with diethyl ether. The solid was dried in vacuum to afford target product as white solid (for the synthesis of compounds **B1**, **C1**-**C6**, **C11**, **D1**-**D19**).

To a solution of above-resulted hydrochloride product in MeOH was added L-tartaric acid, stirred in room temperature for 2 h. After the solvent removal, the residue was washed with diethyl ether, dried in vacuum to afford white solid (for the synthesis of compounds **D20**, **D21**).

After the SAR study, 33 compounds were obtained in total, the compound information of of the target compounds and the intermediates can be found in the following part.

Methyl 3-methyl-5-(1-methyl-1H-pyrazol-5-yl)picolinate (2a)

General procedure A, yield: 94%; ESI-MS: *m/z* = 232 $[M + H]^+$.

Methyl 5-(1-methyl-1H-pyrazol-5-yl)picolinate (2b)

General procedure A, yield: 66%; ^{1}H NMR (500 MHz, $CDCl_3$) δ 8.83 (dd, *J* = 2.2, 0.7 Hz, 1H), 8.23 (dd, *J* = 8.1, 0.7 Hz, 1H), 7.91 (dd, *J* = 8.1, 2.2 Hz, 1H), 7.56 (d, *J* = 2.2 Hz, 1H), 6.45 (d, *J* = 2.2 Hz, 1H), 4.04 (s, 3H), 3.94 (s, 3H). ESI-MS: *m/z* = 218 $[M + H]^+$.

5-(4-Bromo-1-methyl-1H-pyrazol-5-yl)-3-methylpicolinic acid (3a)

General procedure B, yield: 87%; ^{1}H NMR (500 MHz, DMSO-d_6) δ 8.56 (s, 1H), 7.94 (s, 1H), 7.73 (s, 1H), 3.82 (s, 3H), 2.51 (s, 3H). ESI-MS: *m/z* = 294 $[M - H]^-$.

3-Methyl-5-(1-methyl-1H-pyrazol-5-yl)picolinic acid (3b)

General procedure C, yield: 85%; ^{1}H NMR (500 MHz, DMSO- d_6) δ 13.16 (s, 1H), 8.64 (d, *J* = 1.7 Hz, 1H), 7.98 (d, *J* = 1.7 Hz, 1H), 7.54 (d, *J* = 1.9 Hz, 1H), 6.60 (d, *J* = 1.9 Hz, 1H), 3.92 (s, 3H), 2.53 (s, 3H). ESI-MS: *m/z* = 216 $[M - H]^-$.

5-(4-Bromo-1-methyl-1H-pyrazol-5-yl)picolinic acid (3c)

General procedure B, yield: 67%; ^{1}H NMR (500 MHz, DMSO- d_6) δ 13.46 (s, 1H), 8.85 (dd, *J* = 2.0, 1.0 Hz, 1H), 8.21 – 8.15 (m, 2H), 7.76 (s, 1H), 3.84 (s, 3H). ESI-MS: *m/z* = 280 $[M - H]^-$.

Methyl 6-(1-methyl-1H-pyrazol-5-yl)nicotinate (5)

General procedure A, yield: 72%; ^{1}H NMR (500 MHz, $CDCl_3$) δ 9.25 (d, *J* = 2.2 Hz, 1H), 8.31 (dd, *J* = 8.3, 2.2 Hz, 1H), 7.65 (d, *J* = 8.3 Hz, 1H), 7.52 (d, *J* = 1.9 Hz, 1H), 6.68 (d, *J* = 1.9 Hz, 1H), 4.27 (s, 3H), 3.97 (s, 3H). ESI-MS: *m/z* = 218 $[M + H]^+$.

6-(1-Methyl-1H-pyrazol-5-yl)nicotinic acid (6a)

General procedure C, yield: 91%; 1H NMR (500 MHz, DMSO- d_6) δ 9.12 (d, J = 2.1Hz, 1H), 8.31 (dd, J = 8.3, 2.1 Hz, 1H), 7.92 (d, J = 8.3 Hz, 1H), 7.52 (d, J = 1.9 Hz, 1H), 6.92 (d, J = 1.9 Hz, 1H), 4.17 (s, 3H). ESI-MS: m/z = 202 $[M - H]-$.

6-(4-Chloro-1-methyl-1H-pyrazol-5-yl)nicotinic acid (6b)

General procedure B, yield: 88%; ^{1}H NMR (500 MHz, DMSO- d_6) δ 9.20 (d, *J* = 2.2 Hz, 1H), 8.43 (dd, *J* = 8.2, 2.2 Hz, 1H), 7.89 (d, *J* = 8.2, 1H), 7.72 (s, 1H), 3.97 (s, 3H). ESI-MS: *m/z* = 236 $[M - H]^-$.

6-(4-Bromo-1-methyl-1H-pyrazol-5-yl)nicotinic acid (6c)

General procedure B, yield: 94%; ^{1}H NMR (500 MHz, DMSO- d_6) δ 9.20 (d, *J* = 2.2, 0.7 Hz, 1H), 8.43 (dd, *J* = 8.2, 2.2 Hz, 1H), 7.89 (dd, *J* = 8.2, 0.7 Hz, 1H), 7.71 (s, 1H), 3.95 (s, 3H). ESI-MS: *m/z* = 280 $[M - H]^-$.

Methyl 3-chloro-4-(1-methyl-1H-pyrazol-5-yl)benzoate (8a)

General procedure A, yield: 44%; ^{1}H NMR (500 MHz, $CDCl_3$) δ 7.99 (d, *J* = 8.7 Hz, 1H), 7.52 (d, *J* = 1.9 Hz, 1H), 7.38 – 7.23 (m, 2H), 6.34 (d, *J* = 1.9 Hz, 1H), 3.91 (s, 3H), 3.90 (s, 3H). ESI-MS: *m/z* = 251 $[M + H]^+$.

Methyl 3-methyl-4-(1-methyl-1H-pyrazol-5-yl)benzoate (8b)

General procedure A, yield: 97%; ^{1}H NMR (500 MHz, $CDCl_3$) δ 7.99 (s, 1H), 7.92 (dd, *J* = 7.9, 1.3 Hz, 1H), 7.58 (d, *J* = 1.9 Hz, 1H), 7.29 (d, *J* = 7.9 Hz, 1H), 6.25 (d, *J* = 1.9 Hz, 1H), 3.95 (s, 3H), 3.68 (s, 3H), 2.23 (s, 3H). ESI-MS: *m/z* = 231 $[M + H]^+$.

Methyl 4-(1-methyl-1H-pyrazol-5-yl)benzoate (8c)

General procedure A, yield: 89%; ^{1}H NMR (500 MHz, $CDCl_3$) δ 8.12 (d, *J* = 8.3 Hz, 2H), 7.54 (d, *J* = 1.9 Hz, 1H), 7.51 (d, *J* = 8.3 Hz, 2H), 6.38 (d, *J* = 1.9 Hz, 1H), 3.95 (s, 3H), 3.93 (s, 3H). ESI-MS: *m/z* = 217 $[M + H]^+$.

Methyl 2-fluoro-4-(1-methyl-1H-pyrazol-5-yl)benzoate (8d)

General procedure A, yield: 74%; ^{1}H NMR (500 MHz, $CDCl_3$) δ 8.09 – 7.99 (m, 1H), 7.55 (d, *J* = 1.9 Hz, 1H), 7.29 (dd, *J* = 8.1, 1.6 Hz, 1H), 7.23 (dd, *J* = 11.3, 1.6 Hz, 1H), 6.40 (d, *J* = 1.9 Hz, 1H), 3.97 (s, 3H), 3.95 (s, 3H).ESI-MS: *m/z* = 235 $[M + H]^+$.

4-(4-Bromo-1-methyl-1H-pyrazol-5-yl)-3-chlorobenzoic acid (9a)

General procedure B, yield: 53%; ^{1}H NMR (500 MHz, DMSO- d_6) δ 13.62 (s, 1H), 8.12 (d, J = 1.6 Hz, 1H), 8.03 (dd, J = 7.9, 1.6 Hz, 1H), 7.73 (s, 1H), 7.63 (d, J = 7.9 Hz, 1H), 3.65 (s, 3H). ESI-MS: m/z = 313 $[M - H]^-$.

4-(4-Chloro-1-methyl-1H-pyrazol-5-yl)-3-methylbenzoic acid (9b)

General procedure B, yield: 76%; ^{1}H NMR (500 MHz, DMSO- d_6) δ 13.09 (s, 1H), 7.98 (d, J = 6.6 Hz, 1H), 7.93 – 7.83 (m, 1H), 7.69 (s, 1H), 7.44 (d, 7.9 Hz, 1H), 3.58 (s, 3H), 2.18 (s, 3H).ESI-MS: m/z = 249 $[M - H]^-$.

4-(4-Bromo-1-methyl-1H-pyrazol-5-yl)-3-methylbenzoic acid (9c)

General procedure B, yield: 56%; ^{1}H NMR (500 MHz, DMSO- d_6) δ 12.99 (s, 1H), 7.97 (s, 1H), 7.88 (dd, J = 7.9, 1.2 Hz, 1H), 7.69 (s, 1H), 7.39 (d, J = 7.9 Hz, 1H), 3.59 (s, 3H), 2.15 (s, 3H). ESI-MS: m/z = 293 $[M - H]^-$.

4-(4-Chloro-1-methyl-1H-pyrazol-5-yl)benzoic acid (9d)

General procedure B, yield: 94%; ^{1}H NMR (500 MHz, DMSO- d_6) δ 8.11 – 8.08 (m, 2H), 7.70 (s, 1H), 7.68 – 7.64 (m, 2H), 3.80 (s, 3H). ESI-MS: m/z = 235 $[M - H]^-$.

2-Fluoro-4-(1-methyl-1H-pyrazol-5-yl)benzoic acid (9e)

General procedure C, yield: 83%; ^{1}H NMR (500 MHz, DMSO- d_6) δ 13.46 (s, 1H), 8.03 – 7.87 (m, 1H), 7.55 (d, J = 11.8 Hz, 1H), 7.51 (d, J = 1.5 Hz, 1H), 7.49 (d, J = 8.1 Hz, 1H), 6.58 (d, J = 1.5 Hz, 1H), 3.92 (s, 3H). ESI-MS: m/z = 219 $[M - H]^-$.

3-Chloro-4-(1-methyl-1H-pyrazol-5-yl)benzoic acid (9f)

General procedure C, yield: 46%; ^{1}H NMR (500 MHz, DMSO- d_6) δ 13.54 (s, 1H), 8.07 (d, J = 1.7 Hz, 1H), 7.97 (dd, J = 7.9, 1.7 Hz, 1H), 7.62 (d, J = 7.9 Hz, 1H), 7.54 (d, J = 1.9 Hz, 1H), 6.42 (d, J = 1.9 Hz, 1H), 3.66 (s, 3H). ESI-MS: m/z = 235 $[M - H]^-$.

4-(4-Chloro-1-methyl-1H-pyrazol-5-yl)-2-fluorobenzoic acid (9g)

General procedure B, yield: 77%; ^{1}H NMR (500 MHz, DMSO- d_6) δ 13.50 (s, 1H), 8.07 – 7.95 (m, 1H), 7.72 (s, 1H), 7.56 (dd, J = 11.5, 1.5 Hz, 1H), 7.47 (dd, J = 8.0, 1.5 Hz, 1H), 3.82 (s, 3H). ESI-MS: m/z = 253 $[M - H]^-$.

3-Chloro-4-(4-chloro-1-methyl-1H-pyrazol-5-yl)benzoic acid (9h)

General procedure B, yield: 46%; ^{1}H NMR (500 MHz, DMSO- d_6) δ 13.63 (s, 1H), 8.13 (d, J = 1.6 Hz, 1H), 8.04 (dd, J = 7.9, 1.6 Hz, 1H), 7.73 (s, 1H), 7.67 (d, J = 7.9 Hz, 1H), 3.65 (s, 3H). ESI-MS: m/z = 269 $[M - H]^-$.

4-(1-Methyl-1H-pyrazol-5-yl)benzoic acid (9i)

General procedure C, yield: 99%; ^{1}H NMR (500 MHz, $CDCl_3$) δ 8.19 (d, *J* = 8.2 Hz, 2H), 7.61 (d, *J* = 1.8 Hz, 1H), 7.55 (d, *J* = 8.2 Hz, 2H), 6.44 (d, *J* = 1.8 Hz, 1H), 3.99 (s, 3H). ESI-MS: *m/z* = 201 $[M - H]^-$.

4-(4-Bromo-1-methyl-1H-pyrazol-5-yl)benzoic acid (9j)

General procedure B, yield: 94%; ^{1}H NMR (500 MHz, $CDCl_3$) δ 8.26 (d, *J* = 8.3 Hz, 2H), 7.59 (s, 1H), 7.56 (d, *J* = 8.3 Hz, 2H), 3.87 (s, 3H). ESI-MS: *m/z* = 279 $[M - H]^-$.

Tert-butyl (3S,4S)-4-(3-fluorophenyl)-3-nitro-3,4-dihydropyridine-1(2H)-carboxylate (12a)

General procedure D, yield: 47%; ^{1}H NMR (500 MHz, $CDCl_3$) δ 7.35 – 7.28 (m, 1H), 7.19 – 6.93 (m, 4H), 4.93 and 4.82 (d, *J* = 4.3 Hz, and d, *J* = 5.3 Hz, 1H, 1:1.3 ratio due to amide rotamers), 4.69 – 4.59 (m, 1H), 4.26 – 4.22 (m, 1H), 4.17 – 4.06 (m, 1H), 3.92 and 3.99 (d, *J* = 12.5 Hz, and d, *J* = 12.2 Hz, 1H, 1:1.3 ratio due to amide rotamers), 1.52 (s, 9H). ESI-MS: *m/z* = 345 $[M + Na]^+$.

Tert-butyl (3S,4S)-4-(4-chloro-3-(trifluoromethyl)phenyl)-3-nitro-3,4-dihydropyridine-1(2H)-carboxylate (12b)

General procedure D, yield: 72%; ^{1}H NMR (500 MHz, $CDCl_3$) δ 7.56 (d, *J* = 1.9 Hz, 1H), 7.49 (d, *J* = 8.3 Hz, 1H), 7.36 (dd, *J* = 8.3, 1.9 Hz, 1H), 7.18 and 7.03 (d, *J* = 7.9 Hz, and d, *J* = 7.8 Hz, 1H, 1:1.2 ratio due to amide rotamers), 4.89 and 4.78 (d, *J* = 6.0 Hz, and d, *J* = 6.0 Hz, 1H, 1:1.2 ratio due to amide rotamers), 4.66 – 4.58 (m, 1H), 4.29 – 4.26 (m, 1H), 4.11 – 3.97 (m, 2H), 1.53 (s, 9H). ESI-MS: *m/z* = 429 $[M + Na]^+$.

Tert-butyl (3S,4S)-4-(3,4-difluorophenyl)-3-nitro-3,4-dihydropyridine-1(2H)-carboxylate (12c)

General procedure D, yield: 53%; ^{1}H NMR (500 MHz, $CDCl_3$) δ 7.19 – 6.95 (m, 4H), 4.90 and 4.79 (d, *J* = 6.0 Hz, and d, *J* = 5.6 Hz, 1H, 1:1.3 ratio due to amide rotamers), 4.66 – 4.55 (m, 1H), 4.22 – 4.17 (m, 1H), 4.12 – 3.93 (m, 2H), 1.52 (s, 9H). ESI-MS: *m/z* = 363 $[M + Na]^+$.

Tert-butyl (3R,4R)-4-(3-fluorophenyl)-3-nitro-3,4-dihydropyridine-1(2H)-carboxylate (12d)

General procedure D, yield: 58%. ESI-MS: *m/z* = 345 $[M + H]^+$.

Tert-butyl (3S,4S)-4-(3-fluorophenyl)-3-nitropiperidine-1-carboxylate (13a)

General procedure E, yield: 85%; ^{1}H NMR (500 MHz, $CDCl_3$) δ 7.32 – 7.26 (m, 1H), 7.00 – 6.95 (m, 2H), 6.93 – 6.89 (m, 1H), 4.84 – 4.55 (m, 2H), 4.27 (m, 1H), 3.30 (td, *J* = 12.2, 4.1 Hz, 1H), 3.19 (m, 1H), 2.88 (m, 1H), 1.96 (d, *J* = 13.7 Hz, 1H), 1.79 – 1.73 (m, 1H), 1.50 (s, 9H).

Tert-butyl (3S,4S)-4-(4-chloro-3-(trifluoromethyl)phenyl)-3-nitropiperidine-1-carboxylate (13b)

General procedure E, yield: 92%; ^{1}H NMR (500 MHz, $CDCl_3$) δ 7.51 (d, *J* = 2.1 Hz, 1H), 7.46 (d, *J* = 8.3 Hz, 1H), 7.32 (dd, *J* = 8.3, 2.1 Hz, 1H), 4.67 (dd, *J* = 10.6, 7.3 Hz, 1H), 4.31 – 4.28 (m, 1H), 3.78 – 3.71 (m, 1H), 3.38 – 3.31 (m, 1H), 3.29 – 3.07 (m, 1H), 2.90 – 2.87 (m, 1H), 1.95 (d, *J* = 13.5 Hz, 1H), 1.81 – 1.70 (m, 1H), 1.49 (s, 9H).

Tert-butyl (3S,4S)-4-(3,4-difluorophenyl)-3-nitropiperidine-1-carboxylate (13c)

General procedure E, yield: 78%; ESI-MS: *m/z* = 327 $[M - CH_3]^+$.

Tert-butyl (3R,4R)-4-(3-fluorophenyl)-3-nitropiperidine-1-carboxylate (13d)

General procedure E, yield: 70%. ESI-MS: *m/z* = 347 $[M + Na]^+$.

Tert-butyl (3S,4S)-3-amino-4-(3-fluorophenyl)piperidine-1-carboxylate (14a)

General procedure F, yield: 81%; ^{1}H NMR (500 MHz, DMSO- d_6) δ 7.38 (td, J = 7.9, 6.3 Hz, 1H), 7.23 (dd, J = 10.3, 2.0 Hz, 1H), 7.17 (d, J = 7.7 Hz, 1H), 7.10 – 7.06 (m, 1H), 4.37 (d, J = 10.6 Hz, 1H), 4.04 – 3.94 (m, 1H), 3.18 (dd, J = 10.4, 6.5 Hz, 1H), 2.90 – 2.61 (m, 3H), 1.79 – 1.70 (m, 1H), 1.67 – 1.57 (m, 1H), 1.43 (s, 9H). ESI-MS: m/z = 295 [M + H]$^+$.

Tert-butyl (3S,4S)-3-amino-4-(4-chloro-3-(trifluoromethyl)phenyl)piperidine-1-carboxylate (14b)

General procedure F, yield: 96%; ESI-MS: m/z = 379 [M + H]$^+$.

Tert-butyl (3S,4S)-3-amino-4-(3,4-difluorophenyl)piperidine-1-carboxylate (14c)

General procedure F, yield: 89%; ^{1}H NMR (500 MHz, $CDCl_3$) δ 7.15 – 7.09 (m, 1H), 7.05 – 7.01 (m, 1H), 6.97 – 6.93 (m, 1H), 4.45 – 4.09 (m, 2H), 2.92 – 2.67 (m, 2H), 2.56 – 2.43 (m, 1H), 2.38 – 2.29 (m, 1H), 1.76 (d, J = 12.6 Hz, 1H), 1.71 – 1.57 (m, 1H), 1.48 (s, 9H). ESI-MS: m/z = 313 [M + H]$^+$.

Tert-butyl (3R,4R)-3-amino-4-(3-fluorophenyl)piperidine-1-carboxylate (14d)

General procedure F, yield: 99%. ESI-MS: m/z = 295 [M + H]$^+$.

2-Fluoro-N-((3S,4S)-4-(3-fluorophenyl)piperidin-3-yl)benzamide hydrochloride (C1)

General procedure G, yield: 36%; Retention time: 8.931 min, purity: 95.56 %; ^{1}H NMR (500 MHz, MeOD) δ 7.45 (dd, *J* = 12.6, 7.0 Hz, 1H), 7.33 (dd, *J* = 14.1, 6.8 Hz, 2H), 7.15 (t, *J* = 6.5 Hz, 2H), 7.13 – 7.05 (m, 2H), 7.01 – 6.94 (m, 1H), 4.62 (t, *J* = 9.5 Hz, 1H), 3.63 (d, *J* = 9.0 Hz, 1H), 3.53 (d, *J* = 11.2 Hz, 1H), 3.23 – 3.02 (m, 3H), 2.27 – 2.05 (m, 2H). ^{13}C NMR (126 MHz, MeOD) δ 165.35, 163.92, 161.98, 160.57, 158.58, 143.28, 132.80, 130.04, 129.59, 124.10, 122.52, 115.69, 114.26, 48.19, 46.56, 45.09, 43.85, 29.82. HRMS *m/z* (ES+) $[M + H]^+$ = 317.1469 (theor 317.1465).

4-Fluoro-N-((3S,4S)-4-(3-fluorophenyl)piperidin-3-yl)benzamide hydrochloride (C2)

General procedure G, yield: 37%; Retention time: 9.363, purity: 95.29 %; ^{1}H NMR (500 MHz, MeOD) δ 7.65 (dd, *J* = 8.0, 5.3 Hz, 2H), 7.30 (dd, *J* = 13.8, 7.4 Hz, 1H), 7.17 (d, *J* = 7.3 Hz, 1H), 7.10 (t, *J* = 8.5 Hz, 3H), 6.94 (t, *J* = 7.9 Hz, 1H), 4.62 (s, 1H), 3.64 – 3.46 (m, 2H), 3.15 (dd, *J* = 34.0, 23.2 Hz, 3H), 2.15 (dd, *J* = 46.7, 12.4 Hz, 2H). ^{13}C NMR (126 MHz, MeOD) δ 167.31, 165.86, 163.90, 163.87, 161.95, 143.53, 130.10, 129.88, 129.55, 123.32, 115.09, 114.15, 113.81, 48.08, 46.75, 45.09, 43.95, 29.91. HRMS *m/z* (ES+) $[M + H]^+$ = 317.1470 (theor 317.1465).

N-((3S,4S)-4-(3-fluorophenyl)piperidin-3-yl)-2-methoxybenzamide hydrochloride (C3)

General procedure G, yield: 40%; Retention time: 9.161 min, purity: 97.72 %; ^{1}H NMR (500 MHz, MeOD) δ 7.62 (d, *J* = 6.3 Hz, 1H), 7.39 (d, *J* = 36.0 Hz, 2H), 7.14 (t, *J* = 32.8 Hz, 2H), 7.07 – 6.86 (m, 3H), 4.66 (s, 1H), 3.80 (s, 3H), 3.72 (s, 1H), 3.54 (s, 1H), 3.18 (d, *J* = 48.3 Hz, 3H), 2.19 (s, 2H). ^{13}C NMR (126 MHz, MeOD) δ 166.91, 163.96, 162.01, 157.43, 143.56, 132.92, 130.33, 123.56, 121.26, 120.47, 114.40, 113.73, 111.62, 55.97, 48.44, 47.16, 45.19, 44.63, 30.22. HRMS *m/z* (ES+) $[M + H]^+$ = 329.1670 (theor 329.1665).

N-((3S,4S)-4-(3-fluorophenyl)piperidin-3-yl)-5-methylthiophene-2-carboxamide hydrochloride (C4)

General procedure G, yield: 72%; Retention time: 9.306 min, purity: 99.17 %; ^{1}H NMR (500 MHz, MeOD) δ 7.35 (d, *J* = 3.7 Hz, 1H), 7.32 – 7.24 (m, 1H), 7.14 (d, *J* = 7.7 Hz, 1H), 7.09 (d, *J* = 10.1 Hz, 1H), 6.98 – 6.90 (m, 1H), 6.75 – 6.69 (m, 1H), 4.54 (td, *J* = 11.4, 3.9 Hz, 1H), 3.61 – 3.47 (m, 2H), 3.19 (dd, *J* = 15.9, 8.0 Hz, 2H), 3.11 (t, *J* = 11.9 Hz, 1H), 2.44 (s, 3H), 2.10 (ddd, *J* = 24.8, 17.5, 9.6 Hz, 2H). ^{13}C NMR (126 MHz, MeOD) δ 163.75, 162.49, 161.86, 146.13, 143.45, 135.01, 129.99, 129.07, 125.82, 123.06, 113.90, 47.85, 46.74, 44.96, 43.66, 29.90, 14.01. HRMS *m/z* (ES+) $[M + H]^+$ = 319.1278 (theor 319.1280).

N-((3S,4S)-4-(3-fluorophenyl)piperidin-3-yl)-5-methylfuran-2-carboxamide hydrochloride (C5)

General procedure G, yield: 84%; Retention time: 8.816 min, purity: 96.42 %; ^{1}H NMR (500 MHz, MeOD) δ 7.38 – 7.22 (m, 1H), 7.13 (t, *J* = 10.2 Hz, 1H), 7.08 (d, *J* = 10.0 Hz, 1H), 6.96 – 6.85 (m, 2H), 6.12 (d, *J* = 2.9 Hz, 1H), 4.69 – 4.53 (m, 1H), 3.59 – 3.49 (m, 2H), 3.18 (dd, *J* = 23.4, 11.5 Hz, 2H), 3.10 (d, *J* = 11.9 Hz, 1H), 2.29 (s, 3H), 2.10 (dt, *J* = 23.6, 12.4 Hz, 2H). ^{13}C NMR (126 MHz, MeOD) δ 163.88, 161.94, 158.75, 155.76, 145.06, 143.40, 129.90, 123.10, 115.93, 113.93, 108.06, 47.05, 46.68, 44.95, 43.75, 30.03, 12.23. HRMS *m/z* (ES+) $[M + H]^+$ = 303.1513 (theor 303.1509).

N-((3S,4S)-4-(3-fluorophenyl)piperidin-3-yl)-1-methyl-1H-pyrazole-5-carboxamide hydrochloride (C6)

General procedure G, yield: 43%; Retention time: 8.174 min, purity: 98.84 %; ^{1}H NMR (500 MHz, MeOD) δ 7.49 (s, 1H), 7.30 (dt, *J* = 14.4, 7.2 Hz, 1H), 7.16 (d, *J* = 7.2 Hz, 1H), 7.11 (d, *J* = 9.7 Hz, 1H), 6.95 (t, *J* = 8.0 Hz, 1H), 6.66 (s, 1H), 4.60 (s, 1H), 3.93 (s, 3H), 3.62 – 3.52 (m, 2H), 3.24 – 3.12 (m, 3H), 2.16 (dd, *J* = 21.5, 9.2 Hz, 2H). ^{13}C NMR (126 MHz, MeOD) δ 163.89, 161.92, 159.49, 143.37, 136.85, 135.69, 130.09, 123.47, 113.83,

107.20, 47.59, 45.14, 43.91, 37.63, 29.69, 19.17. HRMS *m/z* (ES+) $[M + H]^+$ = 303.1625 (theor 303.1621).

2-Fluoro-N-(4-fluorophenyl)-4-(1-methyl-1H-pyrazol-5-yl)benzamide (C7)

General procedure G, yield: 60%; Retention time: 10.821 min, purity: 100 %; ^{1}H NMR (500 MHz, MeOD) δ 7.84 (t, *J* = 7.6 Hz, 1H), 7.70 (dd, *J* = 7.9, 5.1 Hz, 2H), 7.53 (s, 1H), 7.44 (t, *J* = 10.3 Hz, 2H), 7.10 (t, *J* = 8.5 Hz, 2H), 6.49 (s, 1H), 3.92 (s, 3H). ^{13}C NMR (126 MHz, MeOD) δ 163.24, 160.55, 158.60, 141.84, 138.38, 135.00, 134.30, 130.42, 124.37, 123.58, 122.32, 122.26, 116.19, 115.10, 114.92, 106.56, 36.53. HRMS *m/z* (ES+) $[M + H]^+$ = 314.1108 (theor 314.1105).

2-Fluoro-N-(4-methoxyphenyl)-4-(1-methyl-1H-pyrazol-5-yl)benzamide (C8)

General procedure G, yield: 66%; Retention time: 10.602 min, purity: 98.36 %; ^{1}H NMR (500 MHz, MeOD) δ 7.84 (t, *J* = 7.7 Hz, 1H), 7.61 – 7.56 (m, 2H), 7.52 (t, *J* = 3.1 Hz, 1H), 7.46 – 7.40 (m, 2H), 6.95 – 6.90 (m, 2H), 6.49 (d, *J* = 2.0 Hz, 1H), 3.93 (s, 3H), 3.79 (s, 3H). ^{13}C NMR (126 MHz, MeOD) δ 163.07, 160.55, 158.56, 156.99, 141.83, 138.24, 134.84, 131.08, 130.47, 124.52, 124.01, 123.90, 122.13, 116.11, 113.65, 106.47, 54.49, 36.43. HRMS *m/z* (ES+) $[M + H]^+$ = 326.1302 (theor 326.1305).

N-ethyl-2-fluoro-4-(1-methyl-1H-pyrazol-5-yl)benzamide (C9)

General procedure G, yield: 53%; Retention time: 9.208 min, purity: 98.18 %; ^{1}H NMR (500 MHz, MeOD) δ 7.81 (t, *J* = 7.8 Hz, 1H), 7.51 (d, *J* = 2.0 Hz, 1H), 7.39 (ddd, *J* = 12.9, 9.7, 1.6 Hz, 2H), 6.46 (d, *J* = 2.0 Hz, 1H), 3.91 (s, 3H), 3.44 (q, *J* = 7.3 Hz, 2H), 1.24 (t, *J* = 7.3 Hz, 3H). ^{13}C NMR (126 MHz, MeOD) δ 164.56, 160.72, 158.73, 141.85, 138.22, 134.88, 130.47, 124.39, 123.00, 116.07, 106.45, 36.51, 34.55, 13.43. HRMS *m/z* (ES+) $[M + H]^+$ = 248.1195 (theor 248.1199).

N,N-diethyl-2-fluoro-4-(1-methyl-1H-pyrazol-5-yl)benzamide (C10)

General procedure G, yield: 52%; Retention time: 10.071 min, purity: 96.39 %; ^{1}H NMR (500 MHz, MeOD) δ 7.51 (d, *J* = 2.0 Hz, 1H), 7.47 (d, *J* = 7.1 Hz, 1H), 7.41 (ddd, *J* = 11.8, 9.1, 1.5 Hz, 2H), 6.46 (d, *J* = 2.0 Hz, 1H), 3.91 (s, 3H), 3.60 (q, *J* = 7.1 Hz, 2H), 3.32 (d, *J* = 7.1 Hz, 1H), 3.29 (d, *J* = 7.2 Hz, 1H), 1.27 (t, *J* = 7.1 Hz, 3H), 1.13 (t, *J* = 7.1 Hz, 3H). ^{13}C NMR (126 MHz, MeOD) δ 166.37, 158.91, 156.95, 142.06, 138.06, 133.38, 128.24, 124.75, 115.98, 106.26, 43.38, 39.48, 36.47, 12.84, 11.69. HRMS *m/z* (ES+) $[M + H]^+$ = 276.1517 (theor 276.1512).

(S)-2-fluoro-4-(1-methyl-1H-pyrazol-5-yl)-N-(piperidin-3-yl)benzamide hydrochloride (C11)

General procedure G, yield: 64%; Retention time: 7.555 min, purity: 98.18 %; ^{1}H NMR (500 MHz, MeOD) δ 8.05 (d, *J* = 2.0 Hz, 1H), 7.88 (t, *J* = 7.3 Hz, 1H), 7.55 (d, *J* = 9.6 Hz, 2H), 6.81 (d, *J* = 2.0 Hz, 1H), 4.33 (t, *J* = 10.3 Hz, 1H), 4.06 (s, 3H), 3.57 (dd, *J* = 12.6, 3.5 Hz, 1H), 3.37 (d, *J* = 12.3 Hz, 1H), 3.01 (dd, *J* = 14.0, 8.1 Hz, 2H), 2.11 (dd, *J* = 25.7, 13.8 Hz, 2H), 1.81 (ddd, *J* = 36.6, 25.8, 13.6 Hz, 2H). ^{13}C NMR (126 MHz, MeOD) δ 172.03, 164.51, 160.65, 158.64, 144.44, 135.89, 132.27, 130.92, 116.68, 107.63, 56.95, 46.31, 44.38, 43.50, 36.47, 27.63. HRMS *m/z* (ES+) $[M + H]^+$ = 303.1626 (theor 303.1621).

2-Fluoro-N-((3R,4R)-4-(3-fluorophenyl)piperidin-3-yl)-4-(1-methyl-1H-pyrazol-5-yl)benzamide hydrochloride (B1)

General procedure G, yield: 44%; Retention time: 9.159 min, purity: 97.42 %; ^{1}H NMR (500 MHz, MeOD) δ 7.82 (d, *J* = 1.7 Hz, 1H), 7.52 (t, *J* = 7.5 Hz, 1H), 7.41 – 7.33 (m, 3H), 7.19 (d, *J* = 7.6 Hz, 1H), 7.13 (d, *J* = 9.9 Hz, 1H), 6.99 (td, *J* = 8.5, 2.0 Hz, 1H), 6.63 (d, *J* = 1.6 Hz, 1H), 4.66 (dd, *J* = 11.2, 7.7 Hz, 1H), 3.95 (s, 3H), 3.67 (dd, *J* = 11.9, 3.6 Hz, 1H), 3.55 (d, *J* = 11.9 Hz, 1H), 3.18 (dt, *J* = 24.3, 12.4 Hz, 3H), 2.13 (dd, *J* = 30.0, 17.8

Hz, 2H). ^{13}C NMR (126 MHz, MeOD) δ 164.44, 163.92, 161.98, 160.41, 158.40, 143.48, 136.70, 133.31, 130.49, 130.07, 124.68, 123.31, 116.34, 114.24, 113.74, 107.32, 48.25, 46.49, 45.09, 43.79, 36.45, 29.80. HRMS *m/z* (ES+) $[M + H]^+$ = 397.1844 (theor 397.1840).

5-(4-Bromo-1-methyl-1H-pyrazol-5-yl)-N-((3S,4S)-4-(3-fluorophenyl)piperidin-3-yl)-3-methylpicolinamide hydrochloride (D1)

General procedure G, yield: 66%; Retention time: 9.772 min, purity: 98.80 %; ^{1}H NMR (500 MHz, DMSO- d_6) δ 9.60 (s, 2H), 8.83 (d, J = 9.3 Hz, 1H), 8.50 (d, J = 1.7 Hz, 1H), 7.86 (d, J = 1.5 Hz, 1H), 7.70 (s, 1H), 7.34 (dd, J = 14.3, 7.8 Hz, 1H), 7.11 (d, J = 7.7 Hz, 1H), 7.07 (d, J = 10.2 Hz, 1H), 7.02 (td, J = 8.6, 2.3 Hz, 1H), 4.74 – 4.64 (m, 1H), 3.78 (s, 3H), 3.38 – 3.32 (m, 2H), 3.12 (td, J = 11.8, 3.7 Hz, 1H), 3.01 – 2.87 (m, 2H), 2.24 (s, 3H), 2.12 – 1.95 (m, 2H). ^{13}C NMR (125 MHz, DMSO- d_6) δ 165.28, 162.06 (d, J = 241.5 Hz), 149.93, 146.05, 144.84 (d, J = 7.1 Hz), 140.76, 138.74, 136.93, 132.90, 130.28 (d, J = 8.4 Hz), 125.58, 123.78, 114.33 (d, J = 21.0 Hz), 113.59 (d, J = 20.6 Hz), 93.52, 46.47, 46.22, 44.58, 43.15, 38.51, 29.69, 18.40. HRMS *m/z* (ES+) $[M + H]^+$ = 472.1145 (theor 472.1148).

N-((3S,4S)-4-(3-fluorophenyl)piperidin-3-yl)-3-methyl-5-(1-methyl-1H-pyrazol-5-yl)picolinamide hydrochloride (D2)

General procedure G, yield: 43%; Retention time: 9.028 min, purity: 98.87 %; ^{1}H NMR (500 MHz, DMSO- d_6) δ 9.70 (s, 2H), 8.82 (d, J = 9.3 Hz, 1H), 8.56 (d, J = 1.5 Hz, 1H), 7.91 (d, J = 1.1 Hz, 1H), 7.53 (d, J = 1.7 Hz, 1H), 7.32 (dd, J = 14.3, 7.8 Hz, 1H), 7.10 (d, J = 7.7 Hz, 1H), 7.06 (d, J = 10.2 Hz, 1H), 7.04 – 6.98 (m, 1H), 6.55 (d, J = 1.7 Hz, 1H), 4.68 – 4.61 (m, 1H), 3.86 (s, 3H), 3.37 – 3.30 (m, 2H), 3.17 – 3.08 (m, 1H), 3.02 – 2.85 (m, 2H), 2.23 (s, 3H), 2.13 – 2.05 (m, 1H), 2.01 – 1.94 (m, 1H). ^{13}C NMR (125 MHz, DMSO- d_6) δ 165.01, 162.08 (d, J = 241.4 Hz), 148.59, 144.88 (d, J = 7.1 Hz), 144.44, 139.68, 138.78, 138.16, 133.19, 130.29 (d, J = 8.3 Hz), 127.67, 123.83, 114.37 (d, J = 21.1 Hz), 113.60 (d, J = 20.5 Hz), 107.19, 46.57, 46.22, 44.61, 43.15, 37.78, 29.61, 18.48. HRMS m/z (ES+) $[M + H]^+$ = 394.2047 (theor 394.2043).

N-((3S,4S)-4-(4-chloro-3-(trifluoromethyl)phenyl)piperidin-3-yl)-3-methyl-5-(1-methyl-1H-pyrazol-5-yl)picolinamide hydrochloride (D3)

General procedure G, yield: 67%; Retention time: 10.122 min, purity: 100.00 %; ^{1}H NMR (500 MHz, DMSO- d_6) δ 9.91 – 9.71 (m, 2H), 8.90 (d, J = 9.4 Hz, 1H), 8.55 (d, J =

1.1 Hz, 1H), 7.91 (s, 1H), 7.71 (s, 1H), 7.66 (d, *J* = 8.2 Hz, 1H), 7.60 – 7.54 (m, 1H), 7.54 (s, 1H), 6.55 (d, *J* = 1.4 Hz, 1H), 4.71 – 4.64 (m, 1H), 3.86 (s, 3H), 3.35 (d, *J* = 10.6 Hz, 2H), 3.20 (dd, *J* = 16.3, 7.1 Hz, 1H), 3.05 – 2.84 (m, 2H), 2.23 – 2.10 (m, 4H), 2.05 – 1.94 (m, 1H). ^{13}C NMR (125 MHz, DMSO-*d6*) δ 165.02, 148.51, 144.38, 141.85, 139.67, 138.76, 138.12, 133.28, 133.10, 131.64, 128.98, 127.65, 127.45 (q, *J* = 5.1 Hz), 126.23 (q, *J* = 30.4 Hz), 122.88 (q, *J* = 271.4 Hz), 107.16, 46.59, 46.16, 44.39, 43.06, 37.73, 28.88, 18.22. HRMS *m/z* (ES+) $[M + H]^+$ = 478.1626 (theor 478.1621).

5-(4-Bromo-1-methyl-1H-pyrazol-5-yl)-N-((3S,4S)-4-(3-fluorophenyl)piperidin-3-yl)picolinamide hydrochloride (D4)

General procedure G, yield: 80%; Retention time: 9.598 min, purity: 98.55 %; ^{1}H NMR (500 MHz, DMSO- d_6) δ 9.64 (d, *J* = 9.7 Hz, 1H), 9.52 (d, *J* = 10.1 Hz, 1H), 9.04 (d, *J* = 9.5 Hz, 1H), 8.72 (d, *J* = 1.5 Hz, 1H), 8.12 (dd, *J* = 8.1, 2.0 Hz, 1H), 8.06 (d, *J* = 8.0 Hz, 1H), 7.73 (s, 1H), 7.30 (dd, *J* = 14.3, 7.8 Hz, 1H), 7.09 (dd, *J* = 18.3, 9.0 Hz, 2H), 6.98 (td, *J* = 8.6, 2.2 Hz, 1H), 4.71 – 4.64 (m, 1H), 3.80 (s, 3H), 3.40 – 3.23 (m, 3H), 3.04 (q, *J* = 11.3 Hz, 1H), 2.89 (dd, *J* = 22.6, 11.3 Hz, 1H), 2.10 – 1.97 (m, 2H). ^{13}C NMR (125 MHz, DMSO- d_6) δ 162.87, 162.00 (d, *J* = 241.4 Hz), 149.35, 148.74, 144.84 (d, *J* = 7.0 Hz),

138.96, 138.76, 136.92, 130.27(d, J = 8.3 Hz), 126.80, 123.59, 122.08, 114.11 (d, J = 20.9 Hz), 113.58 (d, J = 20.8 Hz), 93.58, 46.72, 46.03, 44.23, 43.18, 38.51, 29.73. HRMS *m/z* (ES+) $[M + H]^+$ = 458.0995 (theor 458.0992).

N-((3S,4S)-4-(3,4-difluorophenyl)piperidin-3-yl)-6-(1-methyl-1H-pyrazol-5-yl)nicotinamide hydrochloride (D5)

General procedure G, yield: 47%; Retention time: 9.166 min, purity: 100.00 %; ^{1}H NMR (500 MHz, DMSO- d_6) δ 9.74 – 9.58 (m, 2H), 9.25 (d, J = 8.9 Hz, 1H), 8.97 (d, J = 1.9 Hz, 1H), 8.24 (dd, J = 8.3, 2.1 Hz, 1H), 7.85 (d, J = 8.3 Hz, 1H), 7.51 (d, J = 1.9 Hz, 1H), 7.35 – 7.29 (m, 2H), 7.14 (d, J = 4.5 Hz, 1H), 6.87 (d, J = 1.9 Hz, 1H), 4.63 – 4.55 (m, 1H), 4.10 (s, 3H), 3.41 – 3.33 (m, 2H), 3.32 – 3.25 (m, 1H), 3.06 – 2.89 (m, 2H), 2.18 – 2.09 (m, 1H), 2.03 – 1.96 (m, 1H). ^{13}C NMR (125 MHz, DMSO- d_6) δ 163.76, 150.86, 149.16 (dd, J = 243.8, 12.5 Hz), 148.31 (dd, J = 242.5, 12.5 Hz), 147.89, 139.75, 139.70, 137.90, 136.57, 127.71, 124.46, 122.39, 117.33 (d, J =16.3 Hz), 116.69 (d, J =16.3 Hz), 107.93, 47.64, 46.33, 43.89, 43.25, 39.65, 29.00. HRMS *m/z* (ES+) $[M + H]^+$ = 398.1789 (theor 398.1792).

6-(4-Chloro-1-methyl-1H-pyrazol-5-yl)-N-((3S,4S)-4-(3,4-difluorophenyl) piperidin-3-yl)nicotinamide hydrochloride (D6)

General procedure G, yield: 54%; Retention time: 9.801 min, purity: 100.00 %; ^{1}H NMR (500 MHz, DMSO-d_6) δ 9.62 – 9.49 (m, 2H), 9.23 (d, J = 8.9 Hz, 1H), 9.03 (d, J = 1.8 Hz, 1H), 8.30 (dd, J = 8.2, 2.2 Hz, 1H), 7.78 (d, J = 8.2 Hz, 1H), 7.69 (s, 1H), 7.36 – 7.29 (m, 2H), 7.15 (d, J = 4.7 Hz, 1H), 4.65 – 4.57 (m, 1H), 3.92 (s, 3H), 3.43 – 3.34 (m, 2H), 3.27 – 3.21 (m, 1H), 3.04 – 2.91 (m, 2H), 2.16 – 2.07 (m, 1H), 2.00 (d, J = 12.6 Hz, 1H). ^{13}C NMR (125 MHz, DMSO-d_6) δ 163.78, 149.16 (dd, J = 243.8, 12.5 Hz), 148.78, 148.59, 148.30 (dd, J = 243.8, 12.5 Hz), 139.62, 136.73, 136.47, 136.19, 128.64, 124.42, 124.17, 117.34 (d, J =16.3 Hz), 116.51 (d, J =16.3 Hz), 108.59, 47.56, 46.27, 43.88, 43.19, 39.19, 29.08. HRMS m/z (ES+) $[M + H]^+$ = 432.1405 (theor 432.1403).

6-(4-Bromo-1-methyl-1H-pyrazol-5-yl)-N-((3S,4S)-4-(3,4-difluorophenyl) piperidin-3-yl)nicotinamide hydrochloride (D7)

General procedure G, yield: 54%; Retention time: 9.831 min, purity: 98.63 %; ^{1}H NMR (500 MHz, DMSO-d_6) δ 9.68 – 9.53 (m, 2H), 9.27 (d, J = 8.9 Hz, 1H), 9.03 (d, J = 1.7 Hz, 1H), 8.31 (dd, J = 8.2, 2.2 Hz, 1H), 7.78 (d, J = 8.2 Hz, 1H), 7.68 (s, 1H), 7.37 – 7.30 (m,

2H), 7.15 (d, *J* = 4.5 Hz, 1H), 4.66 – 4.58 (m, 1H), 3.90 (s, 3H), 3.42 – 3.34 (m, 2H), 3.28 – 3.22 (m, 1H), 3.05 – 2.91 (m, 2H), 2.18 – 2.06 (m, 1H), 2.04 – 1.97 (m, 1H). ^{13}C NMR (125 MHz, DMSO-d_6) δ 163.77, 149.16 (dd, *J* = 243.8, 12.5 Hz), 149.23, 148.60, 148.30 (dd, *J* = 243.8, 12.5 Hz), 139.65, 138.89, 138.12, 136.12, 128.72, 124.55, 124.43, 117.34 (d, *J* =17.5 Hz), 116.52 (d, *J* =17.5 Hz), 93.53, 47.57, 46.27, 43.87, 43.20, 39.19, 29.09. HRMS *m/z* (ES+) $[M + H]^+$ = 476.0894 (theor 476.0898).

4-(4-Bromo-1-methyl-1H-pyrazol-5-yl)-3-chloro-N-((3S,4S)-4-(3-fluorophenyl) piperidin-3-yl)benzamide hydrochloride (D8)

General procedure G, yield: 59%; Retention time: 10.046 min, purity: 97.09 %; ^{1}H NMR (500 MHz, DMSO-d_6) δ 9.37 (d, *J* = 9.7 Hz, 1H), 9.29 (d, *J* = 9.9 Hz, 1H), 8.91 (d, *J* = 7.7 Hz, 1H), 7.91 (dd, *J* = 12.2, 1.6 Hz, 1H), 7.81 – 7.73 (m, 1H), 7.69 (s, 1H), 7.54 (dd, *J* = 8.0, 1.1 Hz, 1H), 7.34 (dd, *J* = 14.4, 7.1 Hz, 1H), 7.15 – 7.07 (m, 2H), 7.05 – 7.00 (m, 1H), 4.62 – 4.55 (m, 1H), 3.61 (s, 3H), 3.42 – 3.33 (m, 2H), 3.21 – 3.13 (m, 1H), 3.05 – 2.85 (m, 2H), 2.09 – 1.99 (m, 2H). ^{13}C NMR (125 MHz, DMSO-d_6, 1:1 ratio due to atropisomers) δ 163.94, 162.00 (d, *J* = 241.6 Hz), 144.62 (d, *J* = 6.8 Hz), 138.43, 137.77, 136.94, 133.70 and 133.66, 132.84, 130.28 (d, *J* = 8.0 Hz), 129.86, 128.31 and 128.19, 126.40 and

126.26, 123.56, 114.19 (d, J = 21.8 Hz), 113.64 (d, J = 20.6 Hz), 93.93, 47.36, 46.27, 44.35, 43.19, 37.92, 29.42. HRMS *m/z* (ES+) $[M + H]^+$ = 491.0653 (theor 491.0650).

4-(4-Chloro-1-methyl-1H-pyrazol-5-yl)-N-((3S,4S)-4-(3-fluorophenyl)piperidin-3-yl)-3-methylbenzamide hydrochloride (D9)

General procedure G, yield: 55%; Retention time: 9.871 min, purity: 100.00 %; ^{1}H NMR (500 MHz, DMSO-d_6) δ 9.52 (d, J = 9.9 Hz, 1H), 9.41 (d, J = 10.4 Hz, 1H), 8.76 (d, J = 8.9 Hz, 1H), 7.70 (d, J = 14.0 Hz, 1H), 7.65 (s, 1H), 7.63 – 7.59 (m, 1H), 7.36 – 7.29 (m, 2H), 7.14 (d, J = 7.7 Hz, 1H), 7.11 (d, J = 10.1 Hz, 1H), 7.04 – 6.99 (m, 1H), 4.66 – 4.56 (m, 1H), 3.54 (s, 3H), 3.40 – 3.33 (m, 2H), 3.25 – 3.18 (m, 1H), 3.00 – 2.92 (m, 2H), 2.09 (s, 3H), 2.07 – 1.97 (m, 2H). ^{13}C NMR (125 MHz, DMSO-d_6, 1:1 ratio due to atropisomers) δ 165.33, 162.00 (d, J = 241.5 Hz), 144.80 (d, J = 7.1 Hz), 138.01, 137.89 and 137.86, 136.24, 135.23 and 135.21, 130.58, 130.21 (d, J = 8.4 Hz), 129.90, 129.16 and 129.09, 124.90 and 124.81, 123.62 and 123.60, 114.22 (d, J = 19.5 Hz), 113.56 (d, J = 20.5 Hz), 107.95, 47.20 and 47.16, 46.32, 44.36, 43.19, 37.67, 29.42, 18.98 and 18.97. HRMS *m/z* (ES+) $[M + H]^+$ = 427.1696 (theor 427.1701).

4-(4-Bromo-1-methyl-1H-pyrazol-5-yl)-N-((3S,4S)-4-(3-fluorophenyl)piperidin-3-yl)-3-methylbenzamide hydrochloride (D10)

General procedure G, yield: 46%; Retention time: 9.908 min, purity: 98.96 %; ^{1}H NMR (500 MHz, DMSO-d_6) δ 9.43 (s, 1H), 9.32 (s, 1H), 8.73 (d, J = 8.4 Hz, 1H), 7.71 – 7.66 (m, 1H), 7.66 (s, 1H), 7.60 (t, J = 8.8 Hz, 1H), 7.34 (dd, J = 14.4, 7.7 Hz, 1H), 7.29 (dd, J = 7.9, 1.9 Hz, 1H), 7.14 (d, J = 7.7 Hz, 1H), 7.10 (dd, J = 10.4, 1.5 Hz, 1H), 7.04 – 7.00 (m, 1H), 4.65 – 4.55 (m, 1H), 3.55 (s, 3H), 3.40 – 3.35 (m, 2H), 3.22 – 3.16 (m, 1H), 3.02 – 2.88 (m, 2H), 2.08 (s, 3H), 2.06 – 1.99 (m, 2H). ^{13}C NMR (125 MHz, DMSO-d_6, 1:1 ratio due to atropisomers) δ 165.41, 161.02 (d, J = 241.6 Hz), 144.78 (d, J = 6.6 Hz), 139.80, 138.32, 137.83 and 137.80, 135.23 and 135.21, 130.64, 130.59 and 130.57, 130.25 (d, J = 8.1 Hz), 129.13 and 129.03, 124.90 and 124.79, 123.60 (d, J = 2.3 Hz), 114.23 (d, J = 21.6 Hz), 113.60 (d, J = 20.9 Hz), 93.21, 47.19 and 47.15, 46.36, 44.39, 43.21, 37.73, 29.52 and 29.49, 19.07 and 19.05. HRMS *m/z* (ES+) $[M + H]^+$ = 471.1198 (theor 471.1196).

4-(4-Chloro-1-methyl-1H-pyrazol-5-yl)-N-((3S,4S)-4-(3-fluorophenyl)piperidin-3-yl)benzamide hydrochloride (D11)

General procedure G, yield: 81%; Retention time: 9.661 min, purity: 100.00 %; ^{1}H NMR (500 MHz, MeOD) δ 7.75 (d, *J* = 8.4 Hz, 2H), 7.56 (s, 1H), 7.51 (d, *J* = 8.4 Hz, 2H), 7.36 – 7.30 (m, 1H), 7.19 (d, *J* = 7.8 Hz, 1H), 7.15 – 7.11 (m, 1H), 6.99 – 6.94 (m, 1H), 4.70 – 4.62 (m, 1H), 3.77 (s, 3H), 3.66 – 3.62 (m, 1H), 3.55 (d, *J* = 12.8 Hz, 1H), 3.26 – 3.17 (m, 2H), 3.14 (t, *J* = 12.0 Hz, 1H), 2.21 (dd, *J* = 14.5, 2.3 Hz, 1H), 2.15 – 2.05 (m, 1H). ^{13}C NMR (126 MHz, MeOD) δ 169.02, 152.53, 152.43, 151.75, 151.65, 150.57, 150.47, 149.79, 149.70, 140.15, 139.56, 137.98, 135.63, 132.35, 131.00, 128.74, 125.42, 118.50, 118.37, 117.67, 117.53, 110.14, 49.29, 48.04, 46.08, 45.21, 38.65, 31.25. HRMS *m/z* (ES+) $[M + H]^+$ = 413.1547 (theor 413.1544).

2-Fluoro-N-((3S,4S)-4-(3-fluorophenyl)piperidin-3-yl)-4-(1-methyl-1H-pyrazol-5-yl)benzamide hydrochloride (D12)

General procedure G, yield: 61%; Retention time: 9.023 min, purity: 98.63 %; ^{1}H NMR (500 MHz, DMSO-d_6) δ 9.73 (d, *J* = 8.7 Hz, 1H), 9.65 (d, *J* = 10.0 Hz, 1H), 8.57 (d, *J* = 8.8 Hz, 1H), 7.49 (d, *J* = 1.8 Hz, 1H), 7.45 (d, *J* = 11.2 Hz, 1H), 7.41 – 7.33 (m, 3H), 7.12 (d, *J* = 7.7 Hz, 1H), 7.05 (dd, *J* = 17.0, 9.0 Hz, 2H), 6.49 (d, *J* = 1.8 Hz, 1H), 4.63 – 4.55 (m, 1H), 3.85 (s, 3H), 3.44 – 3.30 (m, 2H), 3.11 – 3.05 (m, 1H), 3.00 – 2.85 (m, 2H), 2.17

– 1.98 (m, 2H). ^{13}C NMR (125 MHz, DMSO-d_6) δ 162.86, 162.02 (d, J = 241.5 Hz), 158.72 (d, J = 249.0 Hz), 144.58 (d, J = 7.1 Hz), 140.74 (d, J = 1.6 Hz), 137.95, 133.94 (d, J = 8.9 Hz), 130.19 (d, J = 8.3 Hz), 130.07 (d, J = 3.4 Hz), 124.21 (d, J = 3.0 Hz), 123.65, 123.29 (d, J = 14.9 Hz), 115.80 (d, J = 23.5 Hz), 114.36 (d, J = 21.1 Hz), 113.59 (d, J = 20.6 Hz), 106.78, 47.34, 46.14, 44.52, 43.06, 37.77, 29.22. HRMS *m/z* (ES+) $[M + H]^+$ = 397.1839 (theor 397.1840).

3-Chloro-N-((3S,4S)-4-(4-chloro-3-(trifluoromethyl)phenyl)piperidin-3-yl)-4-(1-methyl-1H-pyrazol-5-yl)benzamide hydrochloride (D13)

General procedure G, yield: 52%; Retention time: 10.395 min, purity: 100.00 %; ^{1}H NMR (500 MHz, DMSO-d_6) δ 9.69 (d, J = 9.2 Hz, 1H), 9.55 (d, J = 10.1 Hz, 1H), 9.11 (d, J = 8.9 Hz, 1H), 7.92 (d, J = 1.3 Hz, 1H), 7.77 (dd, J = 7.7, 1.1 Hz, 2H), 7.65 (d, J = 8.3 Hz, 1H), 7.59 (d, J = 8.0 Hz, 1H), 7.55 – 7.47 (m, 2H), 6.34 (d, J = 1.5 Hz, 1H), 4.66 – 4.58 (m, 1H), 3.60 (s, 3H), 3.41 – 3.29 (m, 3H), 3.03 – 2.91 (m, 2H), 2.21 – 2.10 (m, 1H), 2.03 (d, J = 12.8 Hz, 1H). ^{13}C NMR (125 MHz, DMSO-d_6) δ 163.96, 141.80, 138.82, 137.98, 135.85, 133.08, 132.95, 132.26, 132.15, 131.70, 128.91, 128.30, 127.46 (q, J =

4.9 Hz), 126.24 (q, *J* = 30.4 Hz), 126.20, 122.85 (q, *J* = 271.5 Hz), 107.32, 47.47, 46.21, 43.98, 43.13, 36.83, 28.60. HRMS *m/z* (ES+) $[M + H]^+$ = 497.1119 (theor 497.1123).

4-(4-Chloro-1-methyl-1H-pyrazol-5-yl)-N-((3S,4S)-4-(4-chloro-3-(trifluoromethyl) phenyl)piperidin-3-yl)-3-methylbenzamide hydrochloride (D14)

General procedure G, yield: 77%; Retention time: 10.631 min, purity: 96.58 %; ^{1}H NMR (500 MHz, DMSO-d_6) δ 9.58 (s, 1H), 9.43 (s, 1H), 8.87 (d, *J* = 8.6 Hz, 1H), 7.79 (s, 1H), 7.73 – 7.56 (m, 5H), 7.30 (d, *J* = 7.5 Hz, 1H), 4.67 – 4.54 (m, 1H), 3.53 (s, 3H), 3.46 – 3.26 (m, 3H), 3.06 – 2.89 (m, 2H), 2.21 – 2.00 (m, 5H). ^{13}C NMR (125 MHz, DMSO-d_6, 1:1 ratio due to atropisomers) δ 165.41, 141.79, 137.96, 137.86 and 137.82, 136.24, 135.08 and 135.05, 132.85, 131.65, 130.58 and 130.55, 129.91, 129.09 and 128.98, 128.85, 127.43 (q, *J* = 4.5 Hz), 126.19 (q, *J* = 30.8 Hz), 124.90 and 124.79, 122.80 (q, *J* = 271.4 Hz), 107.93, 47.24 and 47.20, 46.27, 43.96, 43.12, 37.63, 28.70 and 28.65, 18.90. HRMS *m/z* (ES+) $[M + H]^+$ = 511.1276 (theor 511.1279).

4-(4-Chloro-1-methyl-1H-pyrazol-5-yl)-N-((3S,4S)-4-(4-chloro-3-(trifluoromethyl) phenyl)piperidin-3-yl)-2-fluorobenzamide hydrochloride (D15)

General procedure G, yield: 59%; Retention time: 10.468, purity: 95.37 %; ^{1}H NMR (500 MHz, DMSO-d_6) δ 9.64 (d, J = 9.4 Hz, 1H), 9.51 (d, J = 10.4 Hz, 1H), 8.71 (d, J = 8.9 Hz, 1H), 7.73 (d, J = 1.8 Hz, 1H), 7.71 (d, J = 8.3 Hz, 1H), 7.67 (s, 1H), 7.59 (dd, J = 8.4, 1.7 Hz, 1H), 7.47 – 7.42 (m, 2H), 7.36 (dd, J = 7.9, 1.5 Hz, 1H), 4.65 – 4.57 (m, 1H), 3.76 (s, 3H), 3.41 – 3.31 (m, 2H), 3.15 (td, J = 11.9, 3.7 Hz, 1H), 3.02 – 2.85 (m, 2H), 2.18 – 2.08 (m, 1H), 2.03 (d, J = 12.3 Hz, 1H). ^{13}C NMR (125 MHz, DMSO-d_6) δ 162.93, 158.44 (d, J = 249.3 Hz), 141.60, 136.93 (d, J = 1.8 Hz), 136.54, 133.08, 131.68, 131.10 (d, J = 8.9 Hz), 129.99 (d, J = 3.5 Hz), 129.02, 127.41 (q, J = 4.6 Hz), 126.32 (q, J = 30.4 Hz), 125.69 (d, J = 3.3 Hz), 124.43 (d, J = 15.3 Hz), 122.92 (q, J = 271.3 Hz), 117.28 (d, J = 23.5 Hz), 107.84, 47.23, 46.16, 44.28, 43.02, 38.44, 28.83. HRMS *m/z* (ES+) $[M + H]^+$ = 515.1026 (theor 515.1029).

4-(4-Chloro-1-methyl-1H-pyrazol-5-yl)-N-((3S,4S)-4-(4-chloro-3-(trifluoromethyl) phenyl)piperidin-3-yl)benzamide hydrochloride (D16)

General procedure G, yield: 59%; Retention time: 10.505 min, purity: 100.00 %; ^{1}H NMR (500 MHz, DMSO-d_6) δ 9.55 (d, J = 9.5 Hz, 1H), 9.40 (d, J = 10.3 Hz, 1H), 8.90 (d, J = 8.9 Hz, 1H), 7.83 (d, J = 8.2 Hz, 2H), 7.78 (d, J = 0.9 Hz, 1H), 7.70 – 7.64 (m, 2H),

7.60 (d, *J* = 8.2 Hz, 1H), 7.54 (d, *J* = 8.2 Hz, 2H), 4.68 – 4.59 (m, 1H), 3.74 (s, 3H), 3.47 – 3.28 (m, 3H), 3.02 – 2.93 (m, 2H), 2.17 – 2.00 (m, 2H). ^{13}C NMR (125 MHz, DMSO-d_6) δ 165.28, 141.81, 138.01, 136.47, 134.21, 132.95, 131.63, 130.08, 129.42, 128.87, 127.58, 127.28 (q, *J* = 4.1 Hz), 126.26 (q, *J* = 30.4 Hz), 122.82 (q, *J* = 271.3 Hz), 107.50, 47.20, 46.27, 43.97, 43.13, 38.33, 28.83. HRMS *m/z* (ES+) $[M + H]^+$ = 497.1127 (theor 497.1123).

3-Chloro-4-(4-chloro-1-methyl-1H-pyrazol-5-yl)-N-((3S,4S)-4-(3,4-difluorophenyl) piperidin-3-yl)benzamide hydrochloride (D17)

General procedure G, yield: 78%; Retention time: 10.171 min, purity: 100.00 %; ^{1}H NMR (500 MHz, MeOD) δ 7.83 (dd, *J* = 16.2, 1.4 Hz, 1H), 7.73 – 7.66 (m, 1H), 7.55 (s, 1H), 7.47 (dd, *J* = 7.9, 1.7 Hz, 1H), 7.32 – 7.26 (m, 1H), 7.25 – 7.19 (m, 1H), 7.16 (s, 1H), 4.58 (td, *J* = 11.6, 4.2 Hz, 1H), 3.68 – 3.61 (m, 4H), 3.55 (d, *J* = 12.9 Hz, 1H), 3.22 – 3.07 (m, 3H), 2.26 – 2.18 (m, 1H), 2.10 – 2.02 (m, 1H). ^{13}C NMR (125 MHz, MeOD, 1:1 ratio due to atropisomers) δ 167.52, 151.65 (dd, *J* = 257.5, 11.25 Hz), 150.83 (dd, *J* = 257.5, 11.25 Hz), 139.42, 138.20, 138.08, 137.84, 136.25 and 136.17, 134.03 and 134.00, 131.50, 129.86 and 129.62, 127.28 and 127.00, 125.29, 118.52 (d, *J* =17.5 Hz), 117.56

(d, J=17.5 Hz), 111.25, 49.59, 47.97, 46.13, 45.15, 38.25, 31.30. HRMS *m/z* (ES+) [M + H]$^+$ = 465.1064 (theor 465.1060).

4-(4-Chloro-1-methyl-1H-pyrazol-5-yl)-N-((3S,4S)-4-(3,4-difluorophenyl) piperidin -3-yl) benzamide (2R,3R)-2,3-dihydroxysuccinate (D18)

General procedure G, yield: 70%; Retention time: 9.842 min, purity: 100.00 %; 1H NMR (500 MHz, MeOD) δ 7.77 (d, J = 7.9 Hz, 2H), 7.54 (s, 1H), 7.52 (d, J = 7.9 Hz, 2H), 7.29 (dd, J = 11.0, 7.9 Hz, 1H), 7.22 – 7.14 (m, 2H), 4.61 (t, J = 9.2 Hz, 1H), 3.77 (s, 3H), 3.67 – 3.60 (m, 1H), 3.59 – 3.51 (m, 1H), 3.25 – 3.10 (m, 3H), 2.27 – 2.02 (m, 2H). ^{13}C NMR (100 MHz, DMSO-d_6) δ 174.07, 165.35, 149.07 (dd, J = 234.0, 11.0 Hz), 148.17(dd, J = 234.0, 11.0 Hz), 139.75, 138.03, 136.48, 134.44, 130.07, 129.50, 127.54, 124.30, 117.27 (d, J=17.0 Hz), 116.39 (d, J=18.0 Hz), 107.51, 71.88, 47.69, 46.71, 44.29, 43.29, 38.35, 29.90. HRMS *m/z* (ES+) [M + H]$^+$ = 431.1452 (theor 431.1450).

N-((3S,4S)-4-(3,4-difluorophenyl)piperidin-3-yl)-2-fluoro-4-(1-methyl-1H-pyrazol-5-yl)benzamide hydrochloride (D19)

General procedure G, yield: 70%; Retention time: 9.280 min, purity: 100.00 %; ^{1}H NMR (500 MHz, MeOD) δ 7.69 (d, J = 2.2 Hz, 1H), 7.55 (t, J = 7.6 Hz, 1H), 7.42 – 7.35 (m, 2H),

7.31 – 7.25 (m, 1H), 7.25 – 7.20 (m, 1H), 7.18 – 7.14 (m, 1H), 6.56 (d, *J* = 2.2 Hz, 1H), 4.61 – 4.55 (m, 1H), 3.92 (s, 3H), 3.66 (dd, *J* = 12.4, 4.0 Hz, 1H), 3.57 – 3.51 (m, 1H), 3.20 – 3.07 (m, 3H), 2.20 (d, *J* = 12.0 Hz, 1H), 2.11 – 2.02 (m, 1H). HRMS *m/z* (ES+) [M + H]$^+$ = 415.1746 (theor 415.1746).

N-((3S,4S)-4-(3,4-difluorophenyl)piperidin-3-yl)-4-(1-methyl-1H-pyrazol-5-yl)benzamide (2R,3R)-2,3-dihydroxysuccinate (D20)

General procedure G, yield: 51%; Retention time: 9.318 min, purity: 95.52 %; ^{1}H NMR (400 MHz, DMSO-d_6) δ 8.60 (d, *J* = 8.8 Hz, 1H), 7.75 (d, *J* = 8.3 Hz, 2H), 7.58 (d, *J* = 8.3 Hz, 2H), 7.47 (d, *J* = 1.9 Hz, 1H), 7.37 – 7.27 (m, 2H), 7.14 (s, 1H), 6.44 (d, *J* = 1.9 Hz, 1H), 4.56 – 4.46 (m, 1H), 4.14 (s, 2H), 3.84 (s, 3H), 3.42 – 3.36 (m, 2H), 3.14 – 3.04 (m, 1H), 3.03 – 2.86 (m, 2H), 2.01 – 1.95 (m, 2H). ^{13}C NMR (100 MHz, DMSO-d_6) δ 173.92, 165.36, 149.13 (dd, *J* = 244.0, 12.0 Hz), 148.38 (dd, *J* = 244.0, 12.0 Hz), 141.78, 139.70, 138.00, 133.39, 132.94, 128.20, 127.54, 124.27, 117.25 (d, *J* =16.0 Hz), 116.41 (d, *J* =16.0 Hz), 106.31, 71.94, 47.62, 46.63, 44.23, 43.24, 37.66, 29.73. HRMS *m/z* (ES+) [M + H]$^+$ = 397.1843 (theor 397.1840).

4-(4-Bromo-1-methyl-1H-pyrazol-5-yl)-N-((3S,4S)-4-(3,4-difluorophenyl) piperidin-3-yl)benzamide (2R,3R)-2,3-dihydroxysuccinate (D21)

General procedure G, yield: 73%; Retention time: 9.980 min, purity: 95.07 %; ^{1}H NMR (400 MHz, DMSO-d_6) δ 8.64 (d, J = 8.3 Hz, 1H), 7.78 (d, J = 7.8 Hz, 2H), 7.66 (s, 1H), 7.55 (d, J = 7.9 Hz, 2H), 7.41 – 7.27 (m, 2H), 7.14 (s, 1H), 4.51 – 4.42 (m, 1H), 4.07 (s, 2H), 3.75 (s, 3H), 3.43 – 3.28 (m, 2H), 3.13 – 3.02 (m, 1H), 3.00 – 2.82 (m, 2H), 2.08 – 1.89 (m, 2H). ^{13}C NMR (100 MHz, DMSO-d_6) δ 174.22, 165.36, 149.15 (dd, J = 243.0, 11.0 Hz), 148.58 (dd, J = 243.0, 11.0 Hz), 139.82, 139.64, 138.58, 134.48, 130.65, 129.67, 127.47, 124.29, 117.25 (d, J=16.0 Hz), 116.39 (d, J=17.0 Hz), 92.68, 71.84, 47.81, 46.84, 44.37, 43.34, 38.35, 30.07. HRMS m/z (ES+) $[M + H]^+$ = 475.0948 (theor 475.0945).

Cell Culture. Bone Marrow-Derived Macrophages (BMDMs) were flushed from femurs and tibias of C57BL/6J mice.[44] BMDMs were cultured in DMEM (Gibco) supplied with 10% FBS (Gibco), 1% penicillin-streptomycin (Invitrogen) and 20% L929 conditioned media (a source of M-CSF) for 7 days. The purity of adherent macrophages ($F4/80^+$) was more than 90%, analyzed by FACS. RAW264.7 (Murine macrophages cell line) was purchased from Cell Bank of China Science and cultured in DMEM containing 10% FBS.

Drug Screening. RAW264.7 and BMDMs were plated in six-well plates and incubated at 37℃ in 5% CO2. To evaluate the effect of compounds on promoting macrophages M2 polarization. Cells were treated with 300 nM compounds or 20 ng/ml IL-4 (used as a positive control to promote M2 polarization, Peprotech) for 24 h. Macrophages M2 polarization was determined by measuring *Arg1, Mrc1, Fizz1* mRNA level. To evaluate the effect of compounds on inhibiting macrophages M1 polarization. Cells were pre-incubated 50 ng/ml LPS for 24h to induce M1 polarization, then treated with 300 nM compounds for 24 h. Macrophages M1 polarization was determined by measuring *Mcp1, Inos, Tnf-α* mRNA level.

qRT-PCR. Total RNA was extracted using Trizol (Invitrogen) according to manufacturer's procedures. cDNA synthesis was performed using "TransScript One-Step gDNA Removal and cDNA Synthesis SuperMix" kit (Transgen). qRT-PCR was carried out using Applied Biosystems Fast 7500 Real-time PCR instrument with SYBR Premix Ex Taq™ (TAKARA). Primers used are listed in **Table S4**. The results were normalized to housekeeping gene GAPDH.

Pharmacokinetic Study. This study was performed in strict accordance with the Laboratory Animal Management Regulations (State Scientific and Technological Commission Publication No. 8-27 Rev. 2017) and was approved by Zhejiang University Laboratory Animal Center (Hangzhou, China). SD rats (purchased from Zhejiang Academy of Medical Sciences) were administered compound in saline by oral gavage. Venous blood (100 μL) samples were collected at 0, 0.5, 1, 2, 4, 8, and 12 h. Plasma was separated from whole blood by centrifugation and stored at -20 ℃ until analysis. Compound levels were determined using an API4000 + LC/MS system. The C_{max}, T_{max}, $t_{1/2}$ and AUC were evaluated using Analyst 1.5.1.

Animals and EAE Induction. This study was performed in strict accordance with the Laboratory Animal Management Regulations (State Scientific and Technological Commission Publication No. 8-27 Rev. 2017) and was approved by Zhejiang University Laboratory Animal Center (Hangzhou, China). Mice (C57BL/6J, Female, 8-10 weeks) were obtained from SHANGHAI SLAC LABORATORY ANIMAL CO.LTD, housed and fed in a specific pathogen-free animal facility at Experimental Animal Center of Zhejiang University. To induce EAE, 2 mg/ml MOG_{35-55} peptide dissolved in PBS was mixed with

Complete Freund's Adjuvant (Sigma) containing 4 mg/ml heat-killed Mycobacterium tuberculosis (strain H37Ra, BD Biosciences). Then, the mixture was injected subcutaneously into neck (0.1 ml) and both hindlegs (0.05 ml each) of mice. 200 ng Pertussis toxin (List Biological Lab, Inc) was administered intravenously on day 0 and 1 post immunization. Clinical score and body weight were recorded daily. Clinical scoring system: 0 = healthy; 0.5 = limp tail tip; 1 = limp tail; 1.5 = waddling gait with partial tail weakness; 2 = partial hind limb paralysis; 2.5 = unilateral complete hind limb paralysis; 3 = complete bilateral hind limb paralysis; 3.5 = complete hind limb paralysis and partial forelimb paralysis; 4 = tetraplegia; 4.5 = moribund; 5 = death.[45, 46] To determine the therapeutic effect of **D11** on EAE mice, all the compounds were dissolved in saline, 100 mg/kg **D11**, 200 mg/kg **D11**, 10 mg/kg Dexamethasone (DXM) or vehicle (saline) was intraperitoneally administrated daily from day 7 post immunization.

Isolation of Mononuclear Cells. Spleens and dLNs from vehicle or **D11**-treated EAE mice were homogenized in gentleMACS Dissociator (Miltenyi Biotec) to obtain single-cell suspensions. Brains and spinal cords (CNS) from vehicle or **D11**-treated EAE mice were dissected and digested with Collagenase Type IV (Gibco) and separated on

discontinuous 70%/30% Percoll gradients, centrifuged for 30 min at 500×g, 18 °C. The interphase was diluted by transferring to a clean conical tube containing HBSS, then centrifuged for 5 min at 500×g and 18 °C. Mononuclear cells were collected for further FACS analysis.

Flow Cytometry. For cell surface markers staining, cells were incubated with Fluorochrome-labeled antibodies against CD4, CD11b, CD11c, MHC-II (all from BD Biosciences), F4/80, CD86, CD206 (MMR) (all from Biolegend). For intracellular cytokine staining, single cell suspensions from spleens, dLNs and CNS were re-stimulated with 2 μg/ml brefeldin A (Sigma) and 0.1 μg/ml PMA (Sigma) and 0.5 μg/ml ionomycin (Sigma) for 5h. After cell surface markers were stained, cells were fixed and permeabilized with Cytofix/Cytoperm and Perm/Wash buffer (BD Biosciences) according to the manufacturer's instruction. Anti-IFN-γ (Biolegend), and anti-IL-17A (Biolegend) were used for intracellular cytokines staining to determine the proportion of Th1 and Th17 cells. Cells were analyzed by BD FACScaliber flow cytometer. The fluorescence intensity was analyzed by Cell Quest Software.

Histological Analysis. Vehicle or **D11**-treated EAE mice were fixed in 4% paraformaldehyde (PFA) immediately after perfusion with PBS and spinal cords were isolated. For Luxol Fast Blue (LFB) staining, fresh spinal cords were embedded in OCT (Tissue-Tek) and frozen at -80℃. The frozen sections were immersed for 3 h in 0.1% Luxol Fast Blue solution (Solvent Blue 38, Sigma-Aldrich) at 56-60℃. The sections were rinsed in deionized water and differentiation was initiated in 0.05% aqueous lithium carbonate for 10~12 s, followed by termination in multiple immersions in fresh 70% ethanol until gray and white matter could be distinguished. After washed in deionized water, sections were dehydrated in 80% ethanol (1 min), 95% ethanol (2×1 min), 100% ethanol (3 min) and xylene, finally coverslipped. For hematoxylin-eosin (H&E) staining, fresh spinal cords were embedded in paraffin. Paraffin-embedded sections were stained with H&E by Leica ST5010 to estimate inflammation in CNS. Images were acquired using Zeiss LSM510 Meta fluorescence confocal microscope or Leica DM2500 microscope.

Suppression Assays. To evaluate the suppressive capacity of macrophages, BMDMs were treated with 300 nM **D11** in combination with 50 ng/ml LPS (used to promote M1 polarization) or 10 ng/ml IL-4 (used to promote M2 polarization) for 48 h on day 5 of

differentiation, drugs were removed on day 7. Naïve $CD4^+$ T cells were negatively selected using EasySep Mouse Naïve $CD4^+$ T cells Isolation kit (STEMCELL Technologies Inc) then labeled with carboxyfluorescein succinimidyl ester (CFSE) (Biolegend). BMDMs were cocultured with CFSE-labeled naïve $CD4^+$ T cells in the presence of 500 ng/ml anti-CD3 mAb and 500 ng/ml anti-CD28 mAb (Biolegend) at a ratio of 1:1. After 72h, proliferation of $CD4^+$ T cells was determined by FACS.

Statistical Analysis. Independent experiments were carried out at least three times. Data was shown as mean ± S.E.M in the graphs. Results were analyzed using unpaired two-tailed student's t test or One-Way ANOVA.

Microarray analysis. Total RNA were amplified, labeled and purified by using GeneChip® 3' IVT PLUS Reagent Kit (Cat#902416, Affymetrix, Santa Clara, CA, US) / Ovation FFPE WTA System (Cat#3403， NuGEN, San Carlos, CA, US) / Ovation® Pico WTA System V2(Cat#3302， NuGEN, San Carlos, CA, US)and FL-Ovation™ cDNA Biotin Module V2(Cat#4200， NuGEN, San Carlos, CA, US) followed the manufacturer's instructions to obtain biotin labeled cRNA.

Array hybridization and wash was performed using GeneChip® Hybridization, Wash and Stain Kit (Cat#900720, Affymetrix, Santa Clara, CA, US)in Hybridization Oven 645 (Cat#00-0331-220V, Affymetrix, Santa Clara, CA, US)and Fluidics Station 450 (Cat#00-0079, Affymetrix, Santa Clara, CA, US) followed the manufacturer's instructions.

Slides were scanned by GeneChip® Scanner 3000 (Cat#00-00212, Affymetrix, Santa Clara, CA, US) and Command Console Software 4.0 (Affymetrix, Santa Clara, CA, US) with default settings. Raw data were normalized by MAS 5.0/RMA algorithm, Affy packages in R.

Western blotting and ELISA. BMDMs were lysed in buffer (PH= 7.6) containing 1% Triton X-100, 1% phosphatase inhibitor, 1mM PMSF. Protein extracts were electrophoresed by S.D.S-PAGE and transferred to PVDF membrane and probed with primary antibodies. The primary anti-bodies were as follows: anti-AKT, anti-p-AKT(308), anti-p-AKT(473), anti-Arg-1, anti-Ym1, anti-TNF-α, anti-STAT3, anti-p-STAT3(705), anti-STAT6, anti-p-STAT6 (all purchased from Cell Signaling Technology). Appropriate secondary antibodies and ECL were performed to visualize the protein signaling. GAPDH

was used as a loading control. IFN-γ and IL-17A concentration in cell culture supernatants were determined by ELISA kit (DAKEWE).

ASSOCIATED CONTENT

Supporting Information

The Supporting Information is available free of charge on the ACS Publications website at DOI:

Figure S1 showing structures of 28 compounds from in-house library; **Figure S2** showing the expression level of Arg1/Ym1/Tnf-α protein; **Figure S3** showing the mice weight change and serum parameters during 14 days repeated dose toxicity study. **Figure S4** showing the flow cytometry analysis of dendritic cells and Treg cells; **Figure S5** showing the changes of gene expression in the KEGG pathway analysis; **Table S1** listing the gene biomarker expression fold change of the in-house compounds; **Table S2** listing the organ-to-body weight ratio during 14 days repeated dose toxicity study. **Table S3** listing the organ-to-brain weight ratio during 14 days repeated dose toxicity study. **Table S4** listing

the primers used in qRT-PCR; Compound information for the intermediates and target compounds; NMR spectra and HPLC results for the target compounds.

Molecular formula strings (CSV)

AUTHOR INFORMATION

Corresponding Author

*For X. Dong: dongxw@zju.edu.cn

Author Contributions

Q.W. and X.D. conceived the study and analyzed the data. J.C. synthesized the compounds, analyzed the data and drafted the manuscript, Z.Z., J.Z., J.W. and R. G. performed the biological experiments and analyzed the data, W.Z., S.L. and T.T. synthesized the compounds., Y.H., B.Y. and Q.H. conceived the study.

‡ Q.W., J.C. and Z.Z. contributed equally to this work.

Funding Sources

National Natural Science Foundation of China; Public Welfare Technology Research Program of Zhejiang Province; National Major Scientific and Technological Special Project for “Significant New Drugs Development”.

Notes

The authors declare no competing financial interest.

ACKNOWLEDGMENT

We thank Jianyang Pan (Research and Service Center, College of Pharmaceutical Sciences, Zhejiang University) for performing NMR spectrometry for structure elucidation. This work was supported by grant from the National Natural Science Foundation of China (81673294, 81872878, 81741172, 81473226), Public Welfare Technology Research Program of Zhejiang Province (GF18H310002), National Major Scientific and Technological Special Project for “Significant New Drugs Development” (2018ZX09711002-011-023).

ABBREVIATIONS

MS, Multiple sclerosis; EAE, encephalomyelitis; MOG, Myelin Oligodendrocyte Glycoprotein; NBS, N-Bromo Succinimide; NCS, N-Chloro Succinimide; TFA, Trifluoracetic acid; TEA, Triethylamine; HOBt, 1-hydroxybenzotriazole; EDCI, 1-ethyl-3-(3'-dimethylaminopropyl) carbodiimide hydrochloride; DIPEA, N,N-diisopropylethylamine; EA, Ethyl acetate; qRT-PCR, Quantitative real time polymerase chain reaction

REFERENCES

1 Steinman, L. Immunology of relapse and remission in multiple sclerosis. *Annu. Rev. Immunol.* **2014,** 32, 257-281.

2 Dutta, R.; Trapp, B. D. Mechanisms of neuronal dysfunction and degeneration in multiple sclerosis. *Prog. Neurobiol.* **2011,** 93, 1-12.

3 Van, d. V. P.; De Groot, C. J. Staging of multiple sclerosis (MS) lesions: pathology of the time frame of MS. *Neuropath. Appl. Neuro.* **2000,** 26, 2.

4 Bitsch, A.; Schuchardt, J.; Bunkowski, S.; Kuhlmann, T.; Brück, W. Acute axonal injury in multiple sclerosis - correlation with demyelination and inflammation. *Brain* **2000,** 123 (Pt 6), 1174.

5 Pugliatti, M.; Sotgiu, S.; Rosati, G. The worldwide prevalence of multiple sclerosis - clinical neurology and neurosurgery. *Clin. Neurol. Neurosurg.* **2002,** 104, 182-191.

6 Kamm, C. P.; Uitdehaag, B. M.; Polman, C. H. Multiple sclerosis: current knowledge and future outlook. *Eur. Neurol.* **2014,** 72, 132-141.

7 Carrithers, M. D. Update on disease-modifying treatments for multiple sclerosis. *Clin. Ther.* **2014,** 36, 1938-1945.

8 Dendrou, C. A.; Fugger, L.; Friese, M. A. Immunopathology of multiple sclerosis. *Nat. Rev. Immunol.* **2015,** 15, 545-558.

9 Jiang, Z.; Jiang, J. X.; Zhang, G. X. Macrophages: a double-edged sword in experimental autoimmune encephalomyelitis. *Immunol. Lett.* **2014,** 160, 17.

10 Banerjee, S.; Cui, H.; Xie, N.; Tan, Z.; Yang, S.; Icyuz, M.; Thannickal, V. J.; Abraham, E.; Liu, G. miR-125a-5p regulates differential activation of macrophages and inflammation. *J. Biol. Chem.* **2013,** 288, 35428-35436.

11 Lawrence, T.; Natoli, G. Transcriptional regulation of macrophage polarization: enabling diversity with identity. *Nat. Rev. Immunol.* **2011,** 11, 750-761.

12 Rawji, K. S.; Yong, V. W. The benefits and detriments of macrophages/microglia in models of multiple sclerosis. *Clin. Dev. Immunol.* **2013,** 2013, 948976.

13 Martinez, F. O.; Helming, L.; Gordon, S. Alternative activation of macrophages: an immunologic functional perspective. *Annu. Rev. Immunol.* **2009,** 27, 451.

14 Ben-Nun, A.; Kaushansky, N.; Kawakami, N.; Krishnamoorthy, G.; Berer, K.; Liblau, R.; Hohlfeld, R.; Wekerle, H. From classic to spontaneous and humanized models of multiple sclerosis: impact on understanding pathogenesis and drug development. *J. Autoimmun.* **2014,** 54, 33-50.

15 Abourbeh, G.; Thézé, B.; Maroy, R.; Dubois, A.; Brulon, V.; Fontyn, Y.; Dollé, F.; Tavitian, B.; Boisgard, R. Imaging microglial/macrophage activation in spinal cords of experimental autoimmune encephalomyelitis rats by positron emission tomography using the mitochondrial 18 kDa translocator protein radioligand [^{18}F]DPA-714. *J. Neurosci.* **2012,** 32, 5728-5736.

16 Rawji, K. S.; Yong, V. W. The benefits and detriments of macrophages/microglia in models of multiple sclerosis. *Clin. Dev. Immunol.* **2013,** 2013, 948-976.

17 Xu, Y.; He, Z.; Li, Z.; Fang, S.; Zhang, Y.; Wan, C.; Ma, Y.; Lin, P.; Liu, C.; Wang, G. Irgm1 is required for the inflammatory function of M1 macrophage in early experimental autoimmune encephalomyelitis. *J. Leukocyte Biol.* **2016,** 101, 507.

18 Kigerl, K. A.; Gensel, J. C.; Ankeny, D. P.; Alexander, J. K.; Donnelly, D. J.; Popovich, P. G. Identification of two distinct macrophage subsets with divergent effects causing either neurotoxicity or regeneration in the injured mouse spinal cord. *J. Neurosci.* **2009,** 29, 13435-13444.

19 Hucke, S.; Eschborn, M.; Liebmann, M.; Herold, M.; Freise, N.; Engbers, A.; Ehling, P.; Meuth, S. G.; Roth, J.; Kuhlmann, T. Sodium chloride promotes pro-inflammatory macrophage polarization thereby aggravating CNS autoimmunity. *J. Autoimmun.* **2016,** 67, 90-101.

20 Coull, J. A.; Beggs, S.; Boudreau, D.; Boivin, D.; Tsuda, M.; Inoue, K.; Gravel, C.; Salter, M. W.; De, K. Y. BDNF from microglia causes the shift in neuronal anion gradient underlying neuropathic pain. *Nature* **2005,** 438, 1017.

21 Dougherty, K. D.; Dreyfus, C. F.; Black, I. B. Brain-derived neurotrophic factor in astrocytes, oligodendrocytes, and microglia/macrophages after spinal cord injury. *Neurobiol. Dis.* **2000,** 7, 574-585.

22 Shechter, R.; London, A.; Varol, C.; Raposo, C.; Cusimano, M.; Yovel, G.; Rolls, A.; Mack, M.; Pluchino, S.; Martino, G. Infiltrating blood-derived macrophages are vital cells playing an anti-inflammatory role in recovery from spinal cord injury in mice. *PLoS med.* **2009,** 6, e1000113.

23 Schonberg, D. L.; Goldstein, E. Z.; Sahinkaya, F. R.; Wei, P.; Popovich, P. G.; Mctigue, D. M. Ferritin stimulates oligodendrocyte genesis in the adult spinal cord and can be transferred from macrophages to NG2 cells in vivo. *J. Neurosci.* **2012,** 32, 5374-5384.

24 Mikita, J.; Dubourdieucassagno, N.; Deloire, M. S.; Vekris, A.; Biran, M.; Raffard, G.; Brochet, B.; Canron, M. H.; Franconi, J. M.; Boiziau, C. Altered M1/M2 activation patterns of monocytes in severe relapsing experimental rat model of multiple sclerosis. Amelioration of clinical status by M2 activated monocyte administration. *Mult. Scler.* **2011,** 17, 2-15.

25 Weber, M. S.; Prod'Homme, T.; Youssef, S.; Dunn, S. E.; Rundle, C. D.; Lee, L.; Patarroyo, J. C.; Stã¼Ve, O.; Sobel, R. A.; Steinman, L. Type II monocytes modulate T cell-mediated central nervous system autoimmune disease. *Nat. Med.* **2007,** 13, 935-943.

26 Miron, V. E.; Boyd, A.; Zhao, J. W.; Yuen, T. J.; Ruckh, J. M.; Shadrach, J. L.; Van, W. P.; Wagers, A. J.; Williams, A.; Rjm, F. M2 microglia and macrophages drive

oligodendrocyte differentiation during CNS remyelination. *Nat. Neurosci.* **2013,** 16, 1211-1218.

27 MR, K.; C, Z.; N, v. R.; RJ, F. Macrophage-depletion induced impairment of experimental CNS remyelination is associated with a reduced oligodendrocyte progenitor cell response and altered growth factor expression. *Neurobiol.dis.* **2005,** 18, 166-175.

28 Miron, V. E.; Franklin, R. J. M. Macrophages and CNS remyelination. *J. Neurochem.* **2014,** 130, 165-171.

29 Plowright, A. T.; Drowley, L. Phenotypic screening. *Annu. Rep. Med. Chem.* **2017,** 50, 263-299.

30 Warchal, S. J.; Unciti-Broceta, A.; Carragher, N. O. Next-generation phenotypic screening. *Future Med. Chem.* **2016,** 8, 1331-1347.

31 Weng, Q. J.; Wang, J. Y.; Wang, J. J.; Wang, J.; Sattar, F.; Zhang, Z. K.; Zheng, J. H.; Xu, Z. J.; Zhao, M. T.; Liu, X.; Yang, L. J.; Hao, G. F.; Fang, L.; Lu, Q. R.; Yang,

B.; He, Q. J. Lenalidomide regulates CNS autoimmunity by promoting M2 macrophages polarization. *Cell Death Dis.* **2018,** 9, 251-263.

32 Ying, W.; Cheruku, P. S.; Bazer, F. W.; Safe, S. H.; Zhou, B. Y. Investigation of macrophage polarization using bone marrow derived macrophages. *Jove-J. Vis. Exp.* **2013,** 76, e50323.

33 Montalban, X.; Gold, R.; Thompson, A. J.; Otero-Romero, S.; Amato, M. P.; Chandraratna, D.; Clanet, M.; Comi, G.; Derfuss, T.; Fazekas, F.; Hartung, H. P.; Havrdova, E.; Hemmer, B.; Kappos, L.; Liblau, R.; Lubetzki, C.; Marcus, E.; Miller, D. H.; Olsson, T.; Pilling, S.; Selmaj, K.; Siva, A.; Sorensen, P. S.; Sormani, M. P.; Thalheim, C.; Wiendl, H.; Zipp, F. ECTRIMS/EAN guideline on the pharmacological treatment of people with multiple sclerosis. *Eur. J. Neurol.* **2018**, 25, 215-237.

34 Wust, S.; van den Brandt, J.; Tischner, D.; Kleiman, A.; Tuckermann, J. P.; Gold, R.; Luhder, F.; Reichardt, H. M. Peripheral T cells are the therapeutic targets of glucocorticoids in experimental autoimmune encephalomyelitis. *J. Immunol.* **2008**, 180, 8434-8443.

35 Jiang, Z. L.; Jiang, J. X.; Zhang, G. X. Macrophages: A double-edged sword in experimental autoimmune encephalomyelitis. *Immunol. Lett.* **2014,** 160, 17-22.

36 McCormick, S. M.; Heller, N. M. Regulation of macrophage, dendritic cell, and microglial phenotype and function by the SOCS proteins. *Front. Immunol.* **2015,** 6, 549-567.

37 Lang, R.; Patel, D.; Morris, J. J.; Rutschman, R. L.; Murray, P. J. Shaping gene expression in activated and resting primary macrophages by IL-10. *J. Immunol.* **2002,** 169, 2253-2263.

38 Sica, A.; Mantovani, A. Macrophage plasticity and polarization: in vivo veritas. *J. Clin. Invest.* **2012,** 122, 787-795.

39 Draghici, S.; Khatri, P.; Tarca, A. L.; Amin, K.; Done, A.; Voichita, C.; Georgescu, C.; Romero, R. A systems biology approach for pathway level analysis. *Genome Res.* **2007,** 17, 1537-1545.

40 Kanehisa, M.; Goto, S.; Kawashima, S.; Okuno, Y.; Hattori, M. The KEGG resource for deciphering the genome. *Nucleic Acids Res.* **2004,** 32, D277-D280.

41 Vergadi, E.; Ieronymaki, E.; Lyroni, K.; Vaporidi, K.; Tsatsanis, C. Akt signaling pathway in macrophage activation and M1/M2 polarization. *J. Immuno.* **2017,** 198, 1006-1014.

42 Covarrubias, A. J.; Aksoylar, H. I.; Horng, T. Control of macrophage metabolism and activation by mTOR and Akt signaling. *Semin. Immunol.* **2015**, 27, 286-296.

43 Beharka, A. A.; Crowther, J. E.; McCormack, F. X.; Denning, G. M.; Lees, J.; Tibesar, E.; Schlesinger, L. S. Pulmonary surfactant protein A activates a phosphatidylinositol 3-kinase/calcium signal transduction pathway in human macrophages: participation in the up-regulation of mannose receptor activity. *J. Immunol.* **2005**, 175, 2227-2236.

44 Weischenfeldt, J.; Porse, B. Bone marrow-derived macrophages (BMM): isolation and applications. *Csh Protocols* **2008,** 2008, pdb.prot5080.

45 Paterka, M.; Voss, J. O.; Werr, J.; Reuter, E.; Franck, S.; Leuenberger, T.; Herz, J.; Radbruch, H.; Bopp, T.; Siffrin, V.; Zipp, F. Dendritic cells tip the balance towards induction of regulatory T cells upon priming in experimental autoimmune encephalomyelitis. *J. Autoimmun.* **2017,** 76, 108-114.

46 Yang, Q.; Zheng, C.; Cao, J.; Cao, G.; Shou, P.; Lin, L.; Velletri, T.; Jiang, M.; Chen, Q.; Han, Y.; Li, F.; Wang, Y.; Cao, W.; Shi, Y. Spermidine alleviates experimental autoimmune encephalomyelitis through inducing inhibitory macrophages. *Cell Death Differ.* **2016,** 23, 1850-1861.

Table of Contents graphic

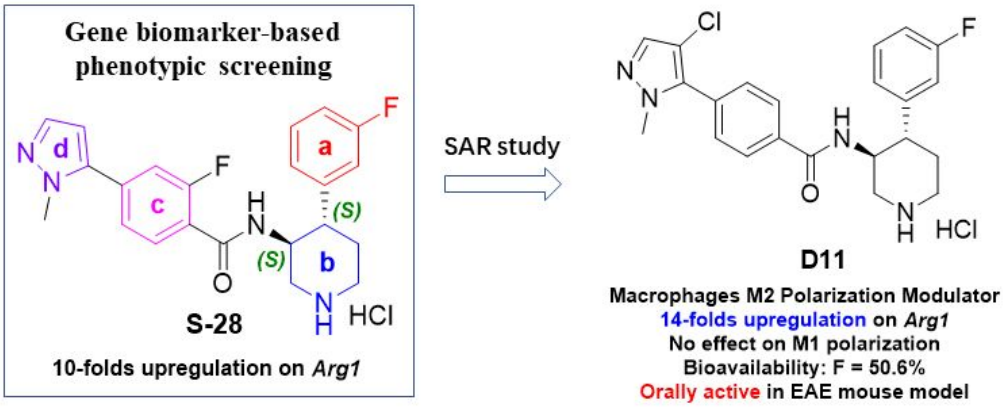

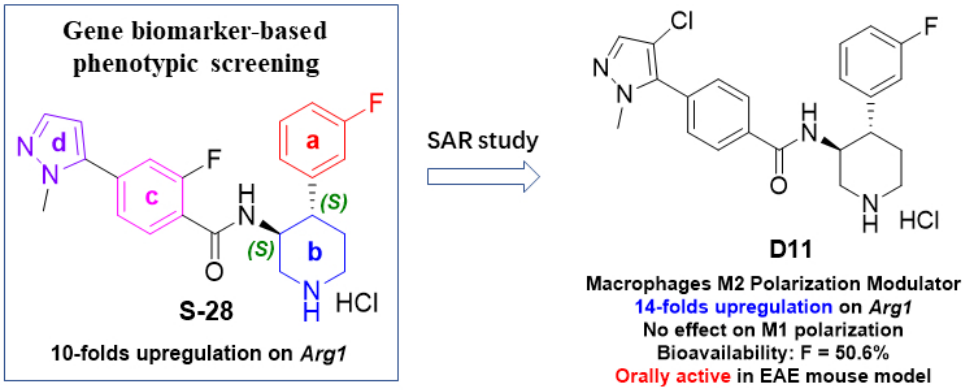

115x50mm (169 x 169 DPI)